MODELING, ANALYSIS AND OPTIMIZATION OF THE THERMAL

PERFORMANCE OF AIR CONDITIONERS

BY

SYED HUSSAIN

A Thesis Presented to the

DEANSHIP OF GRADUATE STUDIES

KING FAHD UNIVERSITY OF PETROLEUM & MINERALS

DHAHRAN, SAUDI ARABIA

In Partial Fulfillment of the
Requirements for the Degree of

MASTER OF SCIENCE

In

MECHANICAL ENGINEERING

MAY 2009

KING FAHD UNIVERSITY OF PETROLEUM AND MINERALS

DHAHRAN 31261, SAUDI ARABIA

DEANSHIP OF GRADUATE STUDIES

This thesis, written by Syed Hussain under the direction of his thesis advisor and approved by his thesis committee, has been presented to and accepted by the Dean of Graduate Studies, in partial fulfillment of the requirements for the degree of **MASTER OF SCIENCE IN MECHANICAL ENGINEERING**.

Thesis Committee

Dr. Esmail M. A. Mokheimer (Advisor)

Dr. Faleh A. Al-Sulaiman (Member)

Dr. Amro M. Al- Qutub (Member)

Dr. Amro M. Al- Qutub

Department Chairman

Dr. Salam A. Zummo

Dean of Graduate Studies

19/10/09

Date

بسم الله الرحمن الرحيم

Dedicated to my beloved

Mother, Father and Sisters

ACKNOWLEDGEMENTS

"In the name of Allah, the Most Beneficent and the Most Merciful"

All praise, glory and thanks are due to Almighty Allah, Most Gracious, and Most Merciful for bestowing me with health, knowledge, opportunity, courage and patience to accomplish this work. May peace and blessings be upon the prophet Muhammad (PBUH), his family and his companions.

Firstly, acknowledgement is due to King Fahd University of Petroleum & Minerals for the support given to purse my graduate studies with financial support and conduct this research through its facilities.

I acknowledge with deep gratitude, the inspiration, encouragement, valuable time, guidance and appreciation given to me by my thesis committee chairman, Dr. Esmail M. A. Mokheimer. I am deeply grateful to Dr. Faleh A. Al-Sulaiman and Dr. Amro M. Al-Qutub, my thesis committee members, for their valuable time, interest, cooperaration and constructive advice.

Special thanks to my seniors at the university Zahid Ilyas, Mohammed Fareeduddin, Razwan Shaik, Mazhar Azim, and Mohammed Omer who always helped me by providing proper guidance. I am thankful to my colleagues Hasan, Mujahid, Sarafaraz, Siraj, Shiraz Bhai, Hafeez Bhai, Murtuza Bhai, Abdur Rahman, Ammar, Asrar, Safdar,

TABLE OF CONTENTS

LIST OF FIGURES

x

LIST OF TABLES

THESIS ABSTRACT (ENGLISH)

NAME: SYED HUSSAIN

TITLE: MODELING, ANALYSIS AND OPTIMIZATION OF THE THERMAL
PERFORMANCE OF AIR CONDITIONERS

MAJOR: MECHANICAL ENGINEERING

DATE: **May 2009**

A large amount of the operating costs in a building is determined by the energy requirements of its air conditioning system. Coupled with the demand for more energy efficient units desired by both manufacturers and consumers, results in a dire necessity to have air conditioning units that are more energy efficient than the existing ones. In order to achieve the above mentioned features, a tool must be designed to simulate the thermal behavior of the air conditioners.

The main objective of this work is to develop a mathematical model for air conditioning unit and coding it into Engineering Equation Solver (EES), a computer program. Once the mathematical model is coded, the thermal performance of three different air conditioning units is evaluated. These air conditioning units are then optimized for maximum Energy Efficiency Ratio (EER) by varying the design parameters by proposing modifications or enhancements in the existing unit. These modifications in the design increase the cost of the air conditioning unit. The AC units indicate an increase of 41.79, 32.52, and 28.24% in the EER corresponding to 38.14, 35.95, and 39.94% increase in the retail cost of AC units I, II, and II respectively. Later, the economics of these modifications is studied based on the measured terms such as the energy savings and the operating cost by evaluating the pay-back-period (PBP). The PBP for the AC units I, II, and III with maximum increase in the EER was evaluated to be 0.91, 0.86, and 1.26 years respectively at an electricity price of 0.2 SAR/kWh. Lastly, the effect of the proposed design modifications on the national economy and environment is evaluated. The results indicate an annual total national energy savings of 25,405.91 GWh, annual total national savings in natural gas (Methane) equivalent to be 5,742.17 million cu. mt, in gasoline and crude oil equivalents to be 40.64 and 38.28 million barrels, in US$ 2,679.61million.

MASTER OF SCIENCE DEGREE

KING FAHD UNIVERSITY OF PETROLEUM and MINERALS

Dhahran, Saudi Arabia

THESIS ABSTRACT (ARABIC)

الاسم: سيد حسين

العنوان: النمذجة والتحليل والتحسين في الأداء الحراري لمكيفات الهواء

التخصص: الهندسة الميكانيكية

التاريخ: مايو 2009

كمية كبيرة من تكاليف التشغيل في مبنى تتحدد من خلال احتياجات الطاقة في نظام تكييف الهواء. إلى جانب الطلب على وحدات أكثر كفاءة للطاقة المرجوة من جانب كل من المنتجين والمستهلكين، وينتج عن ذلك ضرورة ماسة لوحدات تكييف الهواء بحيث تكون أكثر كفاءة في استخدام الطاقة من المحطات القائمة. من أجل تحقيق الميزات المذكورة أعلاه، يجب أن تصميم أداة لمحاكاة السلوك الحراري من مكيفات الهواء.

والهدف الرئيسي من هذا العمل هو تطوير نموذج رياضي لتكييف الهواء وترميزه وتحويله إلى شيفرة   لاستخدامه في برنامج كمبيوتر لحل المعادلات الهندسية . في حال تحويل النموذج الرياضي إلى شيفرة سيتم تقييم الأداء الحراري لثلاث وحدات تكييف مختلفة. هذه الوحدات يتم تصميمها لتكون الأمثل والأعلى في نسبه الكفاءة من خلال التغير في عوامل التصميم من خلال اقتراح تعديلات أو تحسين هذه الوحدات .هذه التعديلات تزيد من تكلفه وحدات التكيف وحدات التكيف تبين زيادة قدرها 41.79 ، 32.52 ، و 28.24 ٪ في نسبه كفاءة الطاقة متوافقة مع 38.14 ، 35.95 ، 39.94 ٪ زيادة في تكلفة وحدات التكييف الأول والثاني ، والثالث على التوالي. في وقت لاحق تم دراسة الجدوى الاقتصادية لهذه التعديلات وفقا للشروط المقاسة مثل تكاليف التشغيل وحفظ الطاقة بتقييم الدفع الخلفي للفترة . الدفع الخلفي للفترة لوحدات التكيف الأولى والثانية والثالثة بالزيادة القصوى لنسبة كفاءة الطاقة وقد تم تقيمها لتكون 0.91، 1.26،0.86 سنويا على التوالي على سعر كهربائي 0.2 ريال لكل كيلو واط /ساعة. أخير تم تقيم الأثر للتعديلات المقترحة على التصميم على الاقتصاد الوطني والبيئة .النتائج تشير الى توفير طاقه كلي وطني سنوي بمقدار 25,405.91 جيجا واط /ساعة، توفير سنوي وطني كلي للغاز الطبيعي الميثان بمقدار5,742.17 مليون متر مكعب، في البنزين والنفط الخام مساوية لـ40.64 و 38.28 مليون برميل والتي تساوي 2,679.61 مليون دولار أمريكي.

درجة الماجستير في العلوم

جامعة الملك فهد للبترول و المعادن

الظهران المملكة العربية السعودية

CHAPTER 1

INTRODUCTION

Air conditioners have become a necessity in many places of the world, particularly where the temperature and humidity are high. One does not feel comfortable if the temperature and humidity level is too high. Air conditioning affects not only personal comfort, but also economics. If people feel comfortable, their productivity is generally better than if, they work under uncomfortable conditions. Thus, air conditioning is and will be more and more needed in our world.

1.1 Motivation for the Present Study

Owing to the rapid development of world economies, the global marketed energy consumption had increased by about 15 percent; i.e. from 366 to 421 quadrillion British Thermal Units (BTU's) over a period of four year (i.e. 1999-2003). It is predicted to further increase by 33.7% in the next decade [1]. Furthermore, during the same period the

electricity consumption is expected to double at the present rate of consumption. Considering the Arabian Gulf; particularly in Kingdom of Saudi Arabia where the electricity consumption has greatly increased, about 75 percent over the past decade. Najim [2] in a symposium presented that the air conditioning equipment consumed about 60 percent of total residential power consumption especially in the long summer season of Saudi Arabia. Saudi Arabia occupies four-fifths of the Arabian Peninsula. Saudi Arabia is the world's 19th greatest electricity consuming nation and accounts for slightly less than 1% of the world annual electricity generation. Electricity generation in Saudi Arabia has also shown a steep rise over the past decade. This increase in the electric generation is always associated with increase in the burning of fossil fuels which possess a grave threat to the environment.

If we take a look at the amount of power generated in the Kingdom of Saudi Arabia (KSA) over a decade we can observe that there has been an increase by 62.3% i.e. from 18,805 MW in the year 1997 to 30,651 MW in 2006 [3] as shown in Figure 1.1. Excluding the energy generated by desalination plants and major producers till 1999. A breakdown of the electricity consumption by the type of sector, during the year 2006 indicates that the residential sector alone contributed for 52.7% of the total electricity consumption in KSA [3] as indicated in Figure 1.2. If we added up the electricity usage for the governmental and commercial sectors to the residential sector, which are all representing loads of buildings, the total building consumption will be about 74% of the total electricity consumption. Hence, it is important to realize the functioning of these

systems in order to have a better understanding over their energy consumption rate enabling us to control the same.
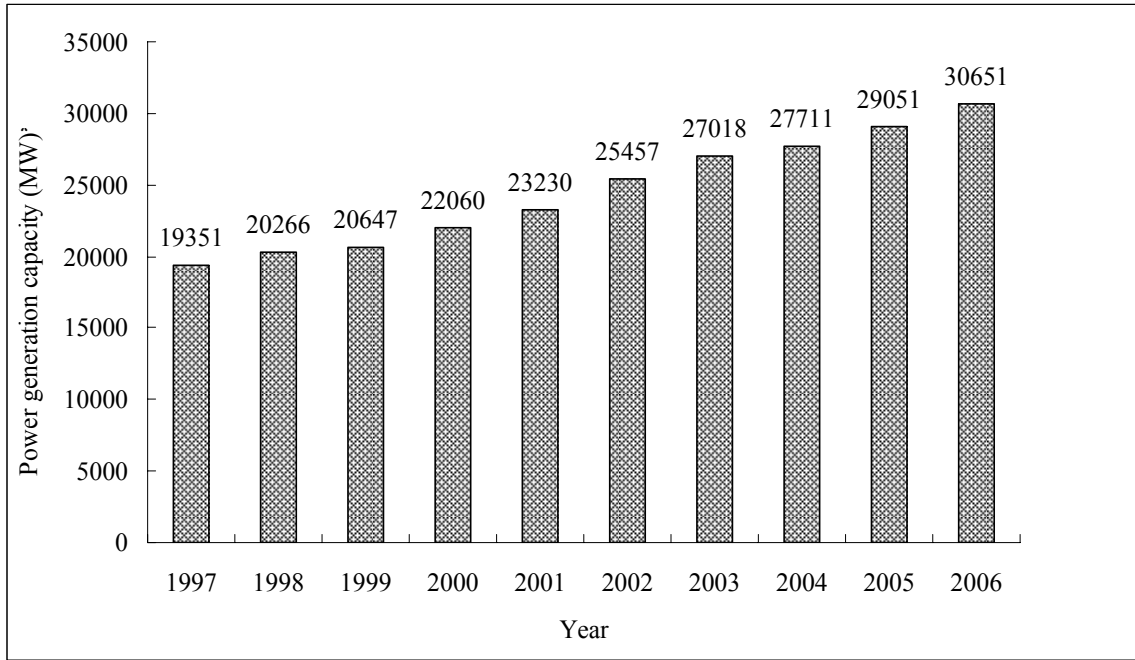
Figure 1.1. Electricity generation over a decade in Saudi Arabia.
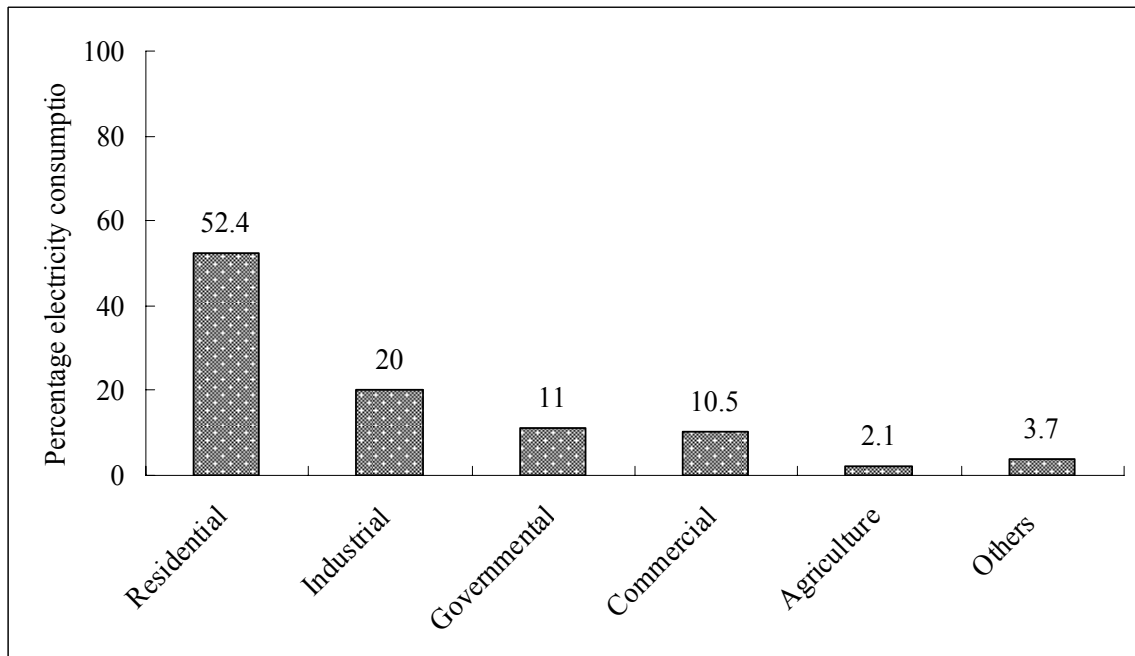
Figure 1.2. Breakdown of electricity consumption in Saudi Arabia during the year 2006.

The demand for designing more energy efficient systems is desired by manufacturers to be able to compete by supplying higher capacity and lower power consumption units. Hence, there is a dire necessity to have air conditioning units that are more energy efficient than the existing ones. For every application; the type of units chosen must compliment its purpose & design considerations. Alongside the installation and functioning of these units must be carried out carefully with utmost engineering accuracy.

The aforementioned requirements have initiated many researches and have led to development of measurement standards such as Energy Efficiency Ratio (EER), Seasonal Energy Efficiency Ratio (SEER), Minimum Energy Performance Standard (MEPS), *etc.* These standards leads us to the concept of optimization, taking into consideration the efficient functioning of the unit from energy consumption point of view; summed up with its correct design and impact on the environment.

Globally, the need for energy efficient air conditioning systems has driven many economies to come up with new strategies. These strategies include setting minimum energy standards on the manufactured products. One such example is the minimum *SEER* set by the United States Department of Energy (*US DOE*) in order to monitor the efficient design and manufacturing of air conditioning units. Obviously, the key to deal with the environmental issues caused by the use of air conditioning units is to raise the energy efficiency of units because it can decrease the demands for fossil fuels since, electricity used to drive these units is mainly derived from burning of fossil fuels and thereby reducing the CO_2 emissions indirectly.

In order to achieve the above-mentioned features, a tool is required to simulate the thermal behavior of the air conditioner. And to calculate this thermal performance under different design options for its components. This simulation tool must be accessible to all and must remain simple enough for wide usage. The development of such a simulation model is the motivation and one of the objectives of the present work. Moreover, the impact of the design options on the national economy and the environment can also be studied.

1.2 Overview

This section deals with an overview of air conditioning and the most commonly used refrigeration cycle i.e. vapor compression cycle. Understanding the basics of the air conditioning process and the fundamentals of the operation of an air conditioner that works on the vapor compression refrigeration cycle is essential before modeling, analyzing or optimizing such machines.

1.2.1 Air Conditioning

Historically, air conditioning has implied cooling or otherwise improving the indoor environment during the warm months of the year. In modern times, the term has taken on a more literal meaning that can be applied to year-round environmental situations. That is, air conditioning refers to the control of temperature, moisture content, cleanliness, odor, and air circulation, as required by the occupants, a process, or product in the space. This general definition has lead to the alternative term 'environmental control'.

The basic components an air conditioning unit incorporates in its casing are; evaporator coil, condenser coil, compressor, expansion valve, and fan. Other components are added based on the size and application requirements such as, humidifier, air distribution system, thermostat, dampers and control systems. These components are assembled in one casing and connected through a refrigerant circuit for supplying air to the environment. Many functions are performed by air conditioning systems by means of cooling, heating, ventilating, humidifying, and de-humidifying air supplied to the conditioned space. Mostly, the operation of these components to give the desired effect to the space is based on the principle of vapor compression refrigeration cycle.

1.2.2 Vapor Compression Cycle

The Vapor Compression Cycle uses energy input to drive a compressor that increases the temperature and pressure of the refrigerant, which is in the vapor state. The refrigerant enters the condenser of the system, its temperature being higher than the ambient surrounding. As a result, heat is transferred from the refrigerant to the ambient environment (i.e. heat is removed from the refrigerant) causing it to condense i.e. for its state to change from the vapor phase to the liquid phase (hence the term condenser). The refrigerant then passes through the expansion device across which its pressure and temperature drop considerably. The refrigerant temperature is now below that of the indoor ambient surrounding of the system. As a result, heat is transferred from the refrigerant in the evaporator causing it to pass from the liquid or near-liquid state to the vapor state again (hence the term evaporator). The refrigerant then again passes to the compressor in which its pressure is again increased and the whole cycle is repeated.

6
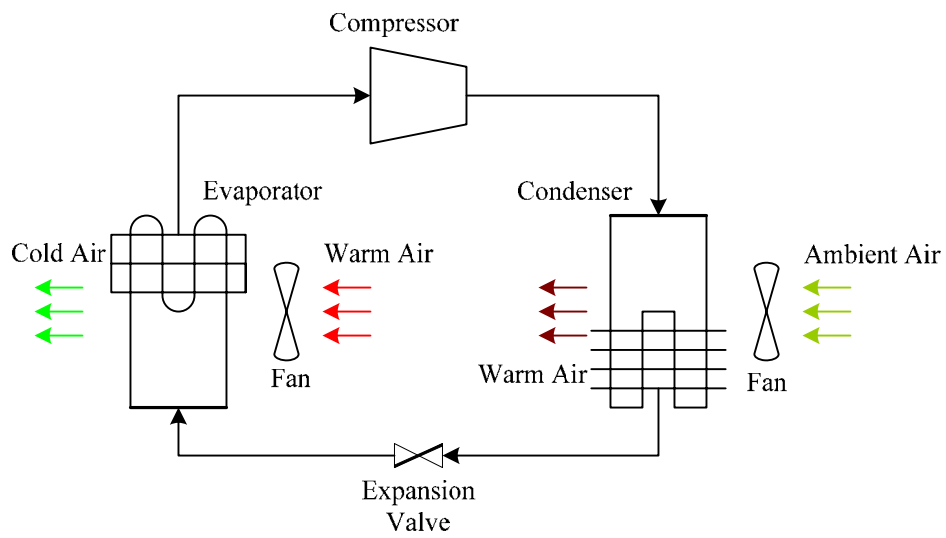
Figure 1.3. Schematic diagram of a typical air conditioner.

Figure 1.4 shows the basic processes in an ideal vapor compression cycle, while the actual vapor compression refrigeration cycle is represented in Figure 1.5 where the dotted lines indicate the ideal cycle.
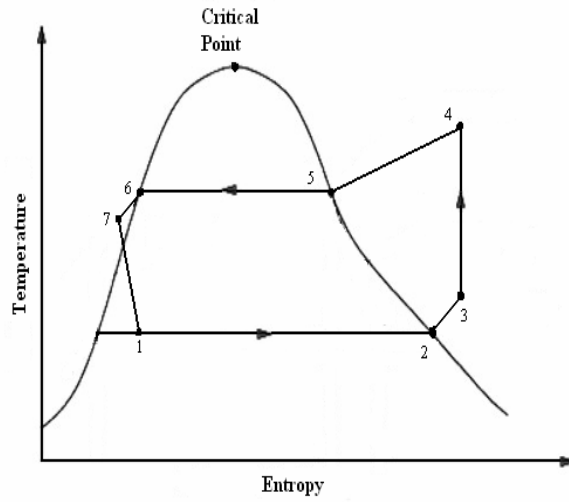
Figure 1.4. Temperature-entropy (T-s) diagram for an ideal vapor compression cycle.
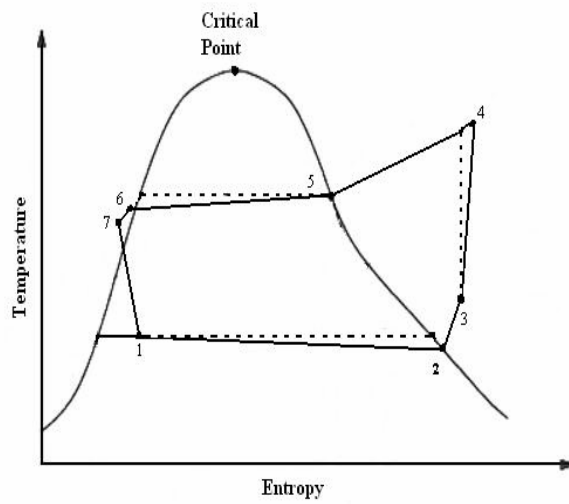
Figure 1.5. Temperature-entropy (T-s) diagram for an actual vapor compression cycle.

The four basic components of the vapor compression refrigeration system are thus:

1. *Evaporator* - Heat is absorbed to boil the liquid at a low temperature, therefore a low pressure must be maintained in this section.

2. *Compressor* - The compressor does work on the system increasing the pressure from that existing in the evaporator (drawing in low- pressure, low-temperature saturated vapor) and to that existing in the condenser (i.e. delivering high pressure and high temperature vapor to the condenser.

3. *Condenser* - The high pressure, high temperature (superheated or saturated) vapor that enters the condenser has heat removed from it and as a result, it is condensed back into a liquid phase.

4. *Throttle valve* - The high pressure liquid from the condenser is expanded through this valve, allowing its pressure to drop to that existing in the evaporator.

CHAPTER 2

LITERATURE REVIEW

The tremendous increase in the energy consumption as well as the global warming motivated a lot of research on energy conservation in general and in particular, the research devoted to the energy efficient air conditioning. In this regard in the past few years, many studies were conducted to investigate energy efficient air conditioning units or energy efficient heat pumps. These studies adopted different approaches for achieving the highly efficient units, by taking into consideration the different components of an air conditioning unit. Out of these various studies, few are enlisted in this section to shed some light in this regard.

Sanaye and Malekmohammadi [4] investigated the thermal and economical optimum design of air conditioning units with vapor compression refrigeration system using the data provided by the manufacturers. They studied the performance of the system under

various rating conditions and implemented the optimization procedure and developed a simulation program which included the thermal and geometrical parameters. The objective function for optimization was the total cost per unit cooling load of the system, which included the capital investment for the various components, as well as the required electricity cost. The objective function was minimized by Lagrange multipliers method in order to find the system design parameters. The effects of changing the cooling load on optimal design parameters were also studied.

Zhang *et al* [5] studied the thermo-economic and thermodynamic optimization of small size central air conditioner by introducing the concept that energy input into the system can be substituted by the sum of energy destruction and energy output from the system according to conservation of energy. They studied the villa air conditioner (VAC) which is more commonly used in China with R134a as the refrigerant. The optimization results indicated that the thermodynamic optimization resulted in reduction in the energy contribution (consumption) and on the other hand the thermo-economic optimization led to a lower life cycle cost. Also the thermodynamic optimization resulted in higher initial investment, which is undesirable for consumers. Operating hours per year and interest rate has different effects on two optimizations. As operating hours increase, life cycle cost at thermodynamic optimization is gradually close to that at thermo economic optimization. However, as interest rate increases, the former gradually deviates from the latter.

Al-Otaibi *et al* [6] performed the thermo economic optimization of vapor compression refrigeration systems and investigated the first law of thermodynamic aspects along with the cost analysis. They developed a model, which included the mass and energy balance equations for the system components along with the cost parameters. The efficiencies of the various components were considered as the decision variables with the cost parameters. The model was then verified by applying it to an R134a vapor compression refrigeration system.

Ding [7] described the recent developments in simulation techniques for vapor compression refrigeration systems as a tool that is widely used for performance evaluation and optimization of the design of refrigeration systems. The models for various components of a refrigeration system were summarized and some developing simulation techniques, including implicit regression and explicit calculation method for refrigerant thermodynamic properties were highlighted. The model-based intelligent simulation methodology and graph-theory based simulation method, were also presented.

Morrison [8] investigated the air conditioner performance rating for different test conditions with compliance to the Australian standards. He made use of simulation technique for the analysis of the performance of the air conditioning systems. The direct assessment of the performance of air conditioner appliances requires access to large capacity calorimeter or psychometric loop test facilities.

The above mentioned research was made considering the air conditioning unit as a single entity, and the effects of the optimizations were presented in the different studies. However, there had been another way of looking at this situation, which considered each of the components in the vapor compression cycle as an individual entity and then integrating their effects in order to obtain the behavior of the complete unit.

2.1 Compressors

Duprez *et. al.* [9] had presented simple and thermodynamically realistic models of two types of compressors widely used in domestic heat pumps (reciprocating and scroll compressors). These models calculate the mass flow rate of refrigerant and the power consumption from the knowledge of operating conditions and parameters. Some of these parameters may be found in the technical datasheets of compressors whereas others are determined in such a way that the calculated mass flow rate and electrical power match those given in these datasheets.

These two models were tested on five reciprocating compressors and five scroll compressors. They studied the compressors with a maximum electrical power of 10 kW under evaporating temperatures ranging from 20 to 15$^\mathrm{o}$ C and condensing temperatures ranging from 15 to 60$^\mathrm{o}$ C. The average errors in mass flow rate and power for reciprocating compressors are 1.10 and 1.69%. And for scroll compressors, the average discrepancies on mass flow rate and power are 2.42 and 1.04%.

Chen *et. al.* [10, 11] developed a comprehensive simulation model of a horizontal scroll compressor, which combined the compression process model and an overall compressor model. In the overall model, compressor components were analyzed in terms of nine different elements. Steady state energy balance equations were established applying the lumped capacitance method. In combination with the detailed compression process model, these equations were implemented into computer code and solved recursively. In this way, the temperature and pressure of the refrigerant in different compressor chambers, the temperature distributions in the scroll wraps, and the temperatures of the other compressor elements were obtained. Thereafter, power consumption and efficiency of the compressor was calculated. Tests were used to verify the overall model on a macroscopic basis. Using the simulation program based on the overall compressor model, a parametric study of the scroll compressor was performed, and the effects of internal leakage and heat transfer losses were investigated and some preliminary results were obtained.

Although the above study presented the means for modeling of the compressor using two approaches: firstly the simple model and the other being the thermodynamically realistic model. The equations governing the parameters cause ambiguity and require detailed analysis of the thermodynamic behavior of the compressor which can remain a hurdle for the wide spread usage for selecting the appropriate compressor. Hence, a simple model must be derived based on the operating parameters of the compressor that can enable in accurate estimation of its performance. The Air-Conditioning and Refrigeration Institute (ARI) [12], which evaluates the performance of a given compressor based on its suction

and discharge temperatures using polynomial expressions, describes one such model. The coefficients of this expression are obtained by curve fitting the performance of the compressor to obtain the desired performance variable.

2.2 Heat Exchangers (Evaporator and Condenser Coils)

Byun *et. al.* [13] performed a numerical analysis of the evaporation performance in a finned tube heat exchanger. They studied the effects of the heat exchanger type, refrigerant, inner tube configuration and fin geometry on evaporator performance by adopting updated correlations, a numerical analysis model based on the tube- by-tube method developed by Domanski [14]. The types of heat exchangers considered were the cross-counter flow type and cross-parallel flow type. The refrigerants investigated for the numerical test as a working fluid were R-134a, R-410A and R-22.

For inner tube configuration, enhanced tube and smooth tube cases was considered. For the air side evaporation performance, heat exchangers using plate fins, wavy fins and slit fins were analyzed. Results depicted that the heat transfer rate of the cross-counter flow type heat exchanger was 3% higher than that of the cross-parallel flow type with R-22. The total heat transfer rate of the evaporator using R-410A was higher than those using R-22 and R-134a, while the total pressure drop of R-410A was lower than those of R-22 and R-134a. The heat transfer rate of the evaporator using enhanced tubes was found to be two times higher than those using smooth tubes, but the pressure drop of the enhanced tube was 45-50% higher than that of the smooth tubes. On the other hand, the evaporation performance of slit fins was superior to that of plate fins by 54%.

Wang *et. al.* [15, 16] proposed a correlation for heat transfer and friction characteristics of a fin and tube heat exchanger having plain geometry. They conducted an experimental evaluation of about 74 samples. Based on the results obtained from these evaluations a correlation for the airside heat transfer coefficient was proposed in terms of dimensionless Coburn *j*-factor taking into consideration the geometric parameters of the heat exchanger. The proposed heat transfer correlation can describe the heat transfer and the air side friction characteristics of a plain fin and tube heat exchanger with a mean deviation of 7.51 and 8.31%, respectively.

In another scenario Wang *et. al.* [17] generalized a correlation for heat transfer and friction for wavy fin geometry from experimental analysis of a total of 27 samples of fin and tube heat exchangers. The correlation that was proposed could predict the heat transfer with a mean deviation of 6.44%, while the proposed friction correlation on the air side could predict the results with a mean deviation of 5.01%.

Similarly, Wang *et. al.* [18] developed a general correlation for airside heat transfer and frictional losses for louvered fin geometry having round tube configuration. A total of 49 samples of louvered fin and tube heat exchangers with different geometric parameters, including louver pitch, louver height, longitudinal tube pitch, transverse tube pitch, tube diameter, and fin pitch were used to develop the correlations. This proposed correlation predicted the performance of the heat exchanger with an accuracy of 95.5% for the Coburn *j*-factor and 90.8% for the air side friction factors within ±15%.

Further, Wang *et. al.* [19] experimentally investigated the airside performance of fin and tube heat exchangers having slit geometry. A total of 12 samples were tested and the effects of fin pitch and the number of tube row was examined. The results indicated that the heat transfer performance increased with decrease of fin pitch for number of longitudinal tube rows, N=1. However, for N≥4, the effect of fin pitch on the heat transfer performance was reversed. Additionally, the heat transfer performance decreased with increase of the number of tube rows and the friction factors were relatively independent. The proposed correlation for the airside performance of the heat exchanger with slit fin configuration described the heat transfer and friction factors with a mean deviation of 5.5 and 3.8%, respectively.

2.3 Throttling Device

Yang and Wang [23] developed a general correlation for predicting the refrigerant mass flow rate through the adiabatic capillary tube with approximate analytic solutions based on data for eight different refrigerants (R12, R22, R134a, R290, R600a, R410A, R407C, and R404A). They employed a homogeneous equilibrium model for two-phase mixture at the inlet of the capillary tube. The database for the capillary tubes covered a range of values for the inner diameter (0.5-2 mm), the tube length (0.5-5 m), the condensing temperature (20-60 ^{o}C), the sub cooling (0-20 ^{o}C), and the refrigerant quality (0-0.3). The refrigerant mass flow rate predicted by the present correlation yields an average deviation of -0.83% and a standard deviation of 9.02% from the experimental data obtained from the open literature and some existing correlations.

17

Choi *et. al.* [25] proposed a general correlation for the refrigerant mass flow rate in adiabatic capillary tubes by implementing dimensionless parameters based on experimental data for three refrigerants (R-22, R-290 and R-407C). These dimensionless parameters were derived from the Buckingham Pi theorem, considering the effects of tube inlet conditions, geometry, and the refrigerant properties on the mass flow rate. The developed correlation was in excellent agreement with the measured data available in the open literature with an average and standard deviations of -0.73 and 6.16% respectively.

Chuan *et. al.* [27] presented the results of experimental data to predict the mass flow rate of R-22 and its alternative refrigerant R-407c through an Electronic Expansion Device (EEV). Based on these experimental results a dimensionless correlation was developed under a series of condensing temperatures, evaporating temperatures, and degrees of sub cooling at the EEV inlet with five open setting degrees of the EEV. The correlation developed was based on the Buckingham Pi theorem with the average and standard deviations of -0.79% and 5.02% for R-22 and 0.67% and 8.08% for R-407c, respectively.

 Park *et. al.* [28] investigated the mass flow characteristics of R-22 and R-410A through Electronic Expansion Valves (EEV) to develop an empirical correlation for the prediction of the refrigerant mass flow rates. They measured the mass flow rates through six EEV's by varying the EEV opening, inlet and outlet pressures, and the sub cooling. The mass flow rates of R-410A were compared with those of R-22 at the same test conditions. The correlation developed was obtained by modifying the orifice equation based on the

experimental data. The correlation prediction was in good agreement with the measured

data with an average and standard deviations of 0.76% and 5.9%, respectively.

CHAPTER 3

OBJECTIVES OF THE PRESENT

STUDY

In the manufacturing and designing an air conditioning system for a space or a building, it is necessary to know which system or product would operate the best and still remain the most cost effective. One convenient way for the manufacturers to figure this out is to run computer simulations, in which the whole unit is modeled and the best solution for the system design is obtained. Hence, models must be available that can predict the overall performance of air conditioning equipment under its operating conditions.

The objective of this work is to develop a mathematical model for an air conditioning unit with vapor compression refrigeration. Such a unit has a compressor, condenser, evaporator, expansion device and blower fans as its major components as indicated already. Hence, detailed modeling and matching of the major components along with a thermo-economic study of the air conditioning units to estimate and improve the overall performance as indicated by the system EER is the main focus of this study.

The main objectives of the present study are:

1. To develop a mathematical model for air conditioning units with vapor compression refrigeration.

2. To code the mathematical model into a computer program.

3. To optimize the overall performance of the air conditioning unit by proposing design enhancements.

4. To study the economics of the proposed enhancements by correlating the modification cost to the increase in the EER.

5. To estimate the economic and environmental impact on a national level as a result of the design modifications.

CHAPTER 4

COMPRESSOR MODELING

Compressor is the central component of a vapor compression cycle. It creates the low and high pressures at its two sides (inlet and outlet respectively). This enables the refrigerant to absorb the heat from the low temperature environment and reject it to the high temperature environment. Thus, a model for the compressor is absolutely necessary. The following sections present the different types of compressors that are generally used in air conditioning applications.

4.1 Reciprocating Compressors

Reciprocating compressors are positive displacement compressors. Reciprocating compressors are classified as hermetic, semi-hermetic and open compressors. The number of cylinders in a reciprocating compressor ranges from one up to eight or sometimes even more cylinders. Often more than one compressor is employed to achieve

higher cooling capacities for large systems. If more than one compressor is used in air conditioning units, part load operation can be achieved by turning off one or more compressors. Often, compressors with more than one cylinder are also equipped with an unloading mechanism, which permits the unloading of one or more cylinders to achieve better part load performance.

In both the hermetic and the semi-hermetic compressors, the motor and the compressor are mounted in a single housing. While the main difference between a hermetic and a semi-hermetic compressor is that the semi-hermetic compressor can be taken apart to do the maintenance work.

4.2 Scroll Compressors

Just like the reciprocating compressors, scroll compressors are also positive displacement compressors. They are employed especially in those systems with a large cooling capacity. This is due to the fact that scroll compressors operate more efficiently than reciprocating compressors. A pictorial and cross-sectional view of a typical scroll compressor is shown in Figure 4.1. In addition, the scroll compressors are more reliable, operate more quietly and smoothly, which makes them increasingly popular for smaller units. The compression process of a scroll compressor is shown in Figure 4.2 [31].
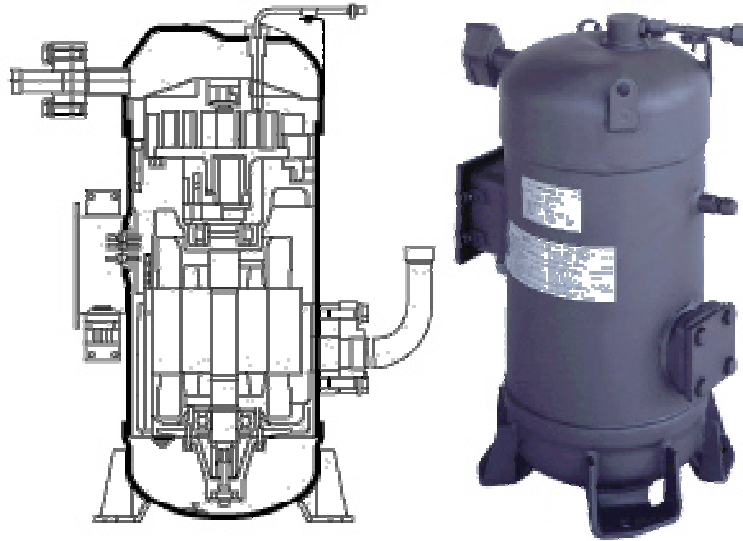
Figure 4.1. Cross-section of a typical scroll compressor.
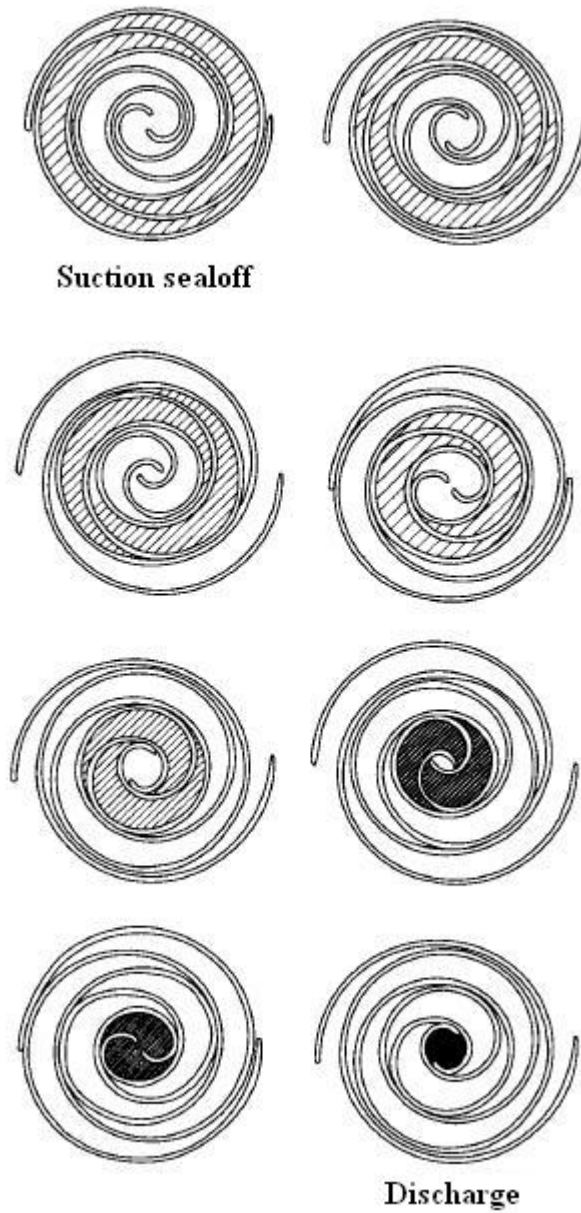
Figure 4.2. Scroll compression process.

The scroll compression process takes place between two scrolls. One scroll is stationary and fixed. The other scroll is assembled with a phase difference of 180° and moves in an orbit around the center of the other scroll. The suction process takes place at the lateral openings. Vapor refrigerant enters the space between the two scrolls. When the orbiting

scroll moves, the space between the two scrolls becomes sealed off and the compression process takes place. The space between the scrolls decreases continuously and by reaching the center of the stationary scroll, the compressed hot refrigerant is discharged through a small opening in the center. Intake, compression, and discharge occur simultaneously in scroll compressors.

4.3 Screw Compressors

A rotary screw compressor is a type of gas compressor which uses a rotary type positive displacement mechanism. The mechanism for compression utilizes either a single screw element or two counter rotating intermeshed helical screw elements housed within a specially shaped chamber. The screw compression element main parts comprise male and female rotors that move towards each other while the volume between them and the housing decreases. As the mechanism rotates, the meshing and rotation of the two helical rotors produces a series of volume-reducing cavities. The effectiveness of this mechanism is dependent on close fitting clearances between the helical rotors and the chamber for sealing of the compression cavities.

A pictorial and schematic view of a typical screw compressor is shown in Figure 4.3. Gas is drawn in through an inlet port in the casing, captured in a cavity, compressed as the cavity reduces in volume, and then discharged through another port in the casing. The screw element is not equipped with any valves and there are no mechanical forces to create any imbalance. It can therefore work at high shaft speed and combine a large flow

26

rate with small exterior dimensions. As a result of which this is the predominant compressor type in use today.
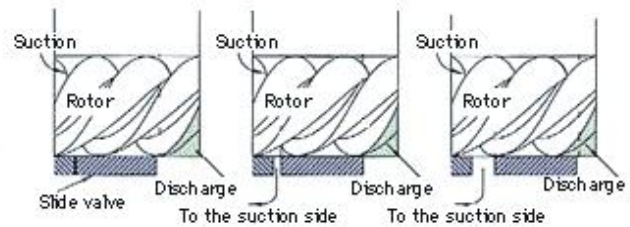
Figure 4.3. Pictographic and Schematic representation of a typical screw compressor.

4.4 Compressor Modeling Approach

It can be inferred from a brief look at the literature from the past few years that, there exists many different techniques to model the compressor. However, there is an inclination towards some while others have just started to emerge as potential options. Simple compressor models, found in thermodynamic textbooks such as Moran and Shapiro [32], often assume the compressor to be adiabatic. Inefficiencies are taken into account by defining isentropic compressor efficiency. More detailed compressor models such as presented by Shapiro [33] also consider heat transfer by developing expressions for the heat loss of the compressor.

Another possibility to describe the performance of compressors is to use polynomial expressions for the mass flow rate, the compressor power drawn and the compressor capacity. Stoecker [34] proposed polynomial expressions for the compressor power draw and the capacity. Each of these expressions contained ten coefficients that have to be determined. Thus, an accurate performance prediction is possible if one has enough data points to determine these coefficients.

For this project, the compressor model described by the Air conditioning and Refrigeration Institute (ARI) [12] is used. The ARI standard uses polynomial expression to derive the compressor performance. The polynomial equation that is used to represent the compressor performance from the experimented tabular data is a third degree equation containing ten coefficients as given hereunder.

$$Y = X_1 + X_2 \cdot (T_S) + X_3 \cdot T_D + X_4 \cdot (T_S^2) + X_5 \cdot (T_S \cdot T_D) + X_6 \cdot (T_D^2) +$$
$$X_7 \cdot (T_S^3) + X_8 \cdot (T_D \cdot T_S^2) + X_9 \cdot (T_S \cdot T_D^2) + X_{10} \cdot (T_D^3) \qquad (3.1)$$

The coefficients X_1-X_{10} represent the compressor performance, which is obtained by curve fitting the performance data. This performance data is obtained from the manufacturer catalogues. The variable 'Y' in the polynomial expression above is a function of the saturated suction temperature and the saturated discharge temperature of the compressor. This variable 'Y' on the left hand side of the polynomial expression can represents the power input, the mass flow rate, the current, the compressor capacity or the compressor unit efficiency. In the present study, equations (3.2) through (3.4) are employed to describe the compressor performance.

28

$$\text{Power}_{\text{comp}} = C_1 + C_2 \cdot (T_S) + C_3 \cdot T_D + C_4 \cdot (T_S^2) + C_5 \cdot (T_S \cdot T_D) + C_6 \cdot (T_D^2) +$$
$$C_7 \cdot (T_S^3) + C_8 \cdot (T_D \cdot T_S^2) + C_9 \cdot (T_S \cdot T_D^2) + C_{10} \cdot (T_D^3)$$

(3.2)

$$\text{Mass}_{\text{comp}} = D_1 + D_2 \cdot (T_S) + D_3 \cdot T_D + D_4 \cdot (T_S^2) + D_5 \cdot (T_S \cdot T_D) + D_6 \cdot (T_D^2) +$$
$$D_7 \cdot (T_S^3) + D_8 \cdot (T_D \cdot T_S^2) + D_9 \cdot (T_S \cdot T_D^2) + D_{10} \cdot (T_D^3)$$

(3.3)

$$Q_{\text{comp}} = E_1 + E_2 \cdot (T_S) + E_3 \cdot T_D + E_4 \cdot (T_S^2) + E_5 \cdot (T_S \cdot T_D) + E_6 \cdot (T_D^2) +$$
$$E_7 \cdot (T_S^3) + E_8 \cdot (T_D \cdot T_S^2) + E_9 \cdot (T_S \cdot T_D^2) + E_{10} \cdot (T_D^3)$$

(3.4)

The work done by the compressor for the above calculated power and mass flow rate is given by equation (3.5). The refrigerant state at the exit of the compressor is evaluated using equation (3.6).

$$W_{comp} = \frac{Power_{comp} \cdot \eta_{mech}}{Mass_{comp}}$$

(3.5)

$$h_4 = h_3 + W_{comp}$$

(3.6)

$$EER_{comp} = \frac{Q_{comp}}{Power_{comp}}$$

(3.7)

where η_{mech} is the mechanical efficiency of the compressor and EER_{comp} is the energy

efficiency ratio of the compressor.

CHAPTER 5

<u>HEAT EXCHANGER MODELING</u>

The process of heat exchange between two fluids that are at different temperatures and separated by a solid wall occurs in many engineering applications. The device used to implement this exchange is termed as a "*heat exchanger*". Heat exchangers are classified in various ways. Sometimes the heat transfer process is used to identify the heat exchanger *i.e.,* direct vs. indirect exchangers. Compactness is another means of classifications. Also, flow arrangements, construction types, fluid flow process and heat transfer mechanisms are used to classify heat exchangers. Many types of exchangers are developed and used in air conditioning, space heating, heat and power plants, process industries, gas turbine systems, electronics cooling, waste heat recovery *etc.* In most exchangers, the heat transfer is due to convection and conduction from a hot to a cold fluid which are separated by solid walls.

Design and sizing of heat exchangers involve many complex procedures. The total amount of heat transferred, pressure drop, performance efficiency, manufacturing and operating costs are important in the final design process. In some cases, the overall cost is more important while in other applications weight and size are the most vital factors.

Thus, it is of great interest to predict the performance of heat exchangers. Many models have been developed for predicting the performance of different kinds of heat exchangers by using different modeling techniques.

A simple way of modeling heat exchangers is to fit a polynomial expression to measured performance data similar to that in case of a compressor. The form of these polynomial curve-fits depends on the type of heat exchanger. Stoecker [34] proposed polynomials for a variety of heat exchangers such as cooling coils and condensers. Depending on the type of heat exchanger, the form of the polynomial expression and the number of curve fit parameters varies significantly. Using polynomial expressions often requires a large number of known operating points in order to predict the performance accurately.

Common methods to describe heat exchanger performance are the log-mean temperature-difference (LMTD) method and the effectiveness-number of transfer units (ε-NTU) method, which can be found in heat transfer textbooks such as Incropera and de Witt [38]. These methods can take the design and the flow arrangement of the heat exchanger into account. In order to predict performance, the overall heat transfer coefficient is

needed, which can be calculated from fundamental heat and mass transfer relations, knowing the geometry of the heat exchanger.

Often, when predicting the performance with either the LMTD method or the effectiveness-NTU method, the overall heat transfer coefficient is assumed constant. This is done to allow a heat exchanger performance prediction with a low computational effort. However, assuming the overall heat transfer coefficient to be constant leads to considerable deviation in performance prediction if mass flow rates in the heat exchanger vary significantly. Thus, modeling approaches should be used that vary the overall heat transfer coefficient according to the operating conditions.

5.1 Heat Exchangers for Air Conditioning

All air conditioning systems contain at least two heat exchangers, usually called the evaporator and the condenser. In either case, the evaporator or the condenser, the refrigerant flows into the heat exchanger and transfers heat, either gaining or releasing it to the cooling medium. Commonly, the cooling medium is air or water. In the case of the condenser, the hot, high pressure refrigerant gas must be condensed to a sub-cooled liquid.

The condenser accomplishes this by cooling the gas *i.e.*, the refrigerant vapor, transferring its heat to the ambient outdoor air. The cooled refrigerant vapor then condenses into a liquid. However, in the evaporator, the sub-cooled refrigerant flows in,

but the heat flow is reversed, with the relatively cool refrigerant absorbing heat from the relatively hotter indoor air. This cools the air and evaporates the refrigerant which enters the compressor and the cycle is repeated.

For modeling a vapor compression cycle, which is used in many air conditioning applications, models for the evaporator and the condenser are required. Due to different heat transfer mechanisms in the condenser and the evaporator, two different models are used for performance prediction of these two heat exchangers.

Evaporators operate at the lower temperature level of the vapor compression cycle and pick up the refrigeration load. In these cooling coils, the warm air flows across the fins and tubes of the direct expansion coil and is cooled down. The refrigerant enters the cooling coil through an expansion device. This expansion device can be a capillary tube or a thermo-static expansion valve. The latter is typically found in large air conditioning units. The thermo-static expansion valve senses the temperature of the refrigerant as it leaves the evaporator coil and it meters just the correct amount of refrigerant to maintain the predetermined amount of superheat. In units with a low cooling capacity, the capillary tube replaces the expansion valve. The refrigerant enters the direct expansion coil as liquid. As it travels through the coil, picking up heat from the air flowing across the tubes, more and more refrigerant vaporizes. The refrigerant leaves the coil slightly superheated and enters the compressor.

Condensers on the other hand operate at the higher temperature level and reject the heat gained in the vapor compression cycle, which consists of the refrigeration load and the

compressor power, to the ambient. Condensers are either water-cooled condensers, evaporative cooled condensers or air-cooled condensers. Most of the residential air conditioners especially for low and medium size applications employ air-cooled condensers with few exceptions. Air-cooled condensers are used because the air is readily available, first costs are lower, and maintenance costs are reduced. The refrigerant, which is discharged from the compressor at high pressure and temperature, enters the condensing coil as vapor. As the vapor passes through the inside of the tubes, heat is rejected to the ambient, which is at a lower temperature level, and condensation of the refrigerant vapor occurs. Often, sub-cooling of the fully condensed refrigerant occurs in condensing coils.

5.2 Heat Exchanger Modeling Approach

The model for the evaporator and for the condenser coils is based on the effectiveness-NTU method. For sensible heat exchangers such as air-cooled condensers an effectiveness-NTU method is used that is based on temperatures. Whereas for heat exchangers where latent heat transfer occur, such as in cooling coils, an effectiveness-NTU method is used that is based on enthalpies. Both methods are described in the following sections.

5.2.1 Evaporator Modeling Approach

An evaporator is a heat exchanger that works in exactly the opposite manner to that of the condenser. In the evaporator, the sub-cooled refrigerant that entered the expansion

device flows into the heat exchanger as two-phase fluid. The relatively cool refrigerant absorbs the heat from the hotter air which is at the ambient indoor conditions. This transfer of heat cools the air and boils the refrigerant which evaporates into super-heated vapor. The super-heated vapor refrigerant then enters the compressor and completes the cycle. An isometric view of a typical evaporator coil applied in air conditioning applications is shown in Figure 5.1.

The circuiting of the coil is also an important factor that affects the performance of the heat exchanger. The flow direction of the refrigerant with respect to that of the air leads to three different flow configurations. However small the variation, these configurations affect the overall performance of the heat exchanger. The heat exchanger arrangement can now be given as cross-flow, cross-counter flow, or cross-parallel flow. In a cross-flow arrangement it is assumed that the each refrigerant region comes in contact with the outdoor air at the same inlet temperature. For the cross-parallel flow arrangement in the heat exchanger, it is assumed that the superheated region is ahead of the two-phase region and that the sub-cooled region is behind the two-phase. While the cross-counter flow arrangement is exactly the opposite of the cross-parallel.

Figure 5.1. Isometric view of a typical evaporator coil.

5.3 Effectiveness-NTU Method for Dry Cooling Coils & Condensers

Evaporator is modeled using an effectiveness-NTU method, which is usually more convenient for heat exchanger performance prediction than the log-mean-temperature-difference approach (LMTD).
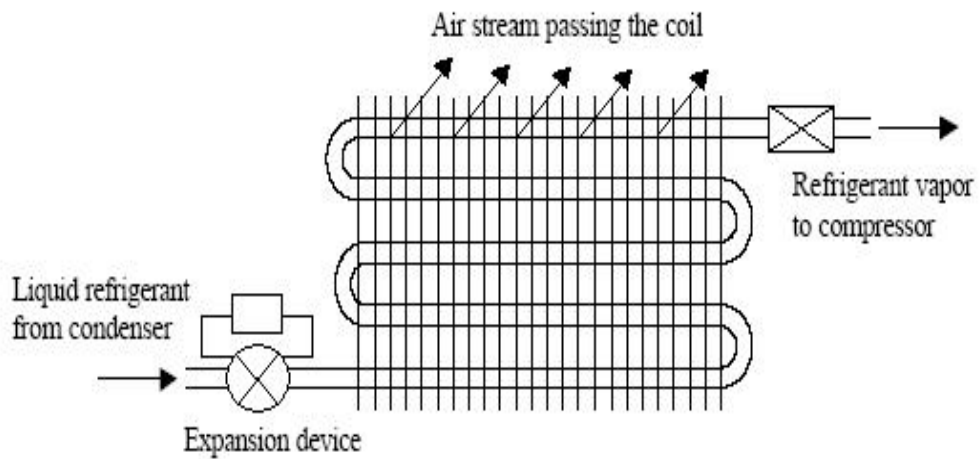
Figure 5.2. Schematic representation of an evaporator coil.

This is due to the fact that, the LMTD method requires the fluid inlet and outlet temperatures. Whereas the effectiveness-NTU method can be applied by just knowing the fluid inlet temperatures. Consequently, obtaining the numerical solution using the LMTD method is often difficult. A schematic representation of an evaporator coil is presented in Figure 5.2. The effectiveness-NTU method is as illustrated below.

The maximum possible heat transfer rate is defined as given by equation (4.1)

$$q_{max,e} = \dot{C}_{min,e}(T_{h,i,e} - T_{c,i,e}) \tag{4.1}$$

where $\dot{C}_{min,e}$ is the minimum capacitance rate. For a direct expansion coil, the capacitance rate of the air is always smaller than the capacitance rate of the refrigerant. Due to the fact that the boiling refrigerant has an effectively infinite specific heat.

The effectiveness of the heat exchanger is defined as the ratio of the actual heat transfer rate to the maximum possible heat transfer rate given by equation (4.2).

$$\varepsilon_e = \frac{q_{act,e}}{q_{max,e}} \tag{4.2}$$

The capacitance rate ratio is defined as the ratio of the minimum capacitance rate to the maximum capacitance rate as given by equation (4.3).

$$\dot{C}_e = \frac{\dot{C}_{min,e}}{\dot{C}_{max,e}} \tag{4.3}$$

The expression for the heat exchanger effectiveness in case of a phase-change fluid is determined by the equation (4.4).

$$\varepsilon_{tp,e} = 1 - \exp(-NTU_{tp,e}) \tag{4.4}$$

This expression for the heat exchanger effectiveness is generally valid for all flow configurations. In the above equation, NTU stands for number of transfer units, which is a dimensionless parameter. The NTU is calculated by dividing the overall heat transfer area coefficient product UA by the minimum capacitance rate as shown in equation (4.5).

$$NTU_{tp,e} = \frac{UA}{\dot{C}_{min,e}} \tag{4.5}$$

The overall heat transfer area product is required to predict the coil performance. The thermal circuit for a coil consists of three thermal resistances. Inside the tube, where the refrigerant passes through, the heat transfer mechanism is convection. The same is true for the air that flows across the finned tubes. The thermal resistance due to conduction through the tube is neglected in calculating the UA product. This is a reasonable assumption, since heat exchanger coils are manufactured of materials with a high thermal conductivity to decrease the thermal resistance due to conduction. The UA product is then calculated by equation (4.6).

$$UA = \cfrac{1}{\cfrac{1}{(\eta_o hA)_a} + \cfrac{1}{(hA)_{ref}}}$$

(4.6)

The heat transfer coefficient on the airside is evaluated from the equations proposed by Wang *et. al.* [15-19] based on the fin pattern. In this regard, they described the heat transfer on the airside based on the Colburn *j*-factor. The Colburn factor is a dimensionless factor in terms of the Nusselt number (*Nu*), Reynolds number (*Re*) and Prandtl number (*Pr*) as given by equation (4.7) and (4.8). The air side heat transfer coefficient is obtained from the equation (4.9) where 'D' is the expanded tube diameter and 'k_{ref}' is the thermal conductivity.

$$j_e = \frac{Nu}{Re.Pr^{1/3}}$$

(4.7)

$$j_e = 0.086 \cdot Re_{D,c,e}{}^{P_{4,i,e}} \cdot a_e{}^{P_{5,i,e}} \cdot \left(\frac{P_{f,e}}{D_{c,e}}\right)^{P_{6,i,e}} \cdot \left(\frac{P_{f,e}}{D_{h,e}}\right)^{P_{7,i,e}} \cdot \left(\frac{P_{f,e}}{P_{T,e}}\right)^{-0.93}$$

(4.8)

$$Nu = \frac{h.D}{k_{ref}}$$

(4.9)

While the evaporation heat transfer coefficient on the refrigerant side is calculated using the expression given by Chaddock and Noerager [40]. The amount of heat transfer from the evaporator is the sum of the heat transfer in the two-phase zone and the super-heated zone as expressed by equation (4.10).

$$Q_{evap,calc} = q_{tp,e} + q_{sh,e}$$

(4.10)

5.4 Effectiveness-NTU Method for Wet Cooling Coils

In all air conditioning systems, cooling coils are used to cool a warm air stream. If the surface temperature of the cooling coil is lower than the dew point temperature of the entering air stream, condensation occurs. In this case, the effectiveness-NTU method for sensible heat exchangers that is based on temperature cannot predict the performance accurately, since the latent heat transfer due to condensation is not taken into account.

Different approaches exist to predict the performance of cooling coils. Empirical models, such as proposed by Stoecker [34], as well as fundamental models exist. Stoecker [34] proposed equations describing the performance of direct expansion cooling coils. Bourdouxhe *et. al.* [35] presented in the HVAC1KIT, that the performance of direct expansion coils is predicted by replacing the air stream by a fictitious water stream. Two models are used. One model describes the coil performance by treating the coil as a heat exchanger where no condensation occurs. The other model describes the performance of the wet coil where condensation occurs. Both models use effectiveness-NTU relationships. The model that predicts the higher heat transfer is chosen for actual performance prediction.

Ritchler [36] presented the expressions for the effectives and NTU such that the capacitance rates and temperatures in the effectiveness-NTU method for sensible heat exchangers are replaced in the analogy approach for wet coils by mass flow rates and enthalpies. The capacitance rates and temperatures in the effectiveness-NTU method for sensible heat exchangers are replaced in the analogy approach for wet coils by mass flow

rates and enthalpies. In the analogy approach the maximum possible heat transfer is calculated similar to the effectiveness-NTU for sensible heat exchanger. Thus, the maximum heat transfer rate is obtained as the product of the minimum capacitance rate, which is the mass flow rate of the air, and the difference between the enthalpy of the entering air and the enthalpy of saturated air at the refrigerant inlet temperature as represented in equation (4.11).

$$Q_{max} = \dot{m}_{a,e} \cdot (h_{a,i} - h_{a,sat,r})$$ (4.11)

Subsequently, the NTU^* and the effectiveness for the wet coil can be calculated by using the effectiveness-NTU relationships given by equations (4.12) and (4.13).

$$NTU^* = \frac{U^* A}{\dot{m}_{a,e}}$$ (4.12)

$$\varepsilon_{tp,e} = 1 - e^{-NTU^*}$$ (4.13)

The enthalpy of the outlet air can be calculated from the expression for the actual heat transfer rate given by equations (4.14) to (4.16).

$$Q_{tp,act} = \varepsilon_{tp,e} \cdot Q_{tp,max}$$ (4.14)

$$Q_{tp,act} = \dot{m}_{a,e} \cdot (h_{a,i} - h_{a,o})$$ (4.15)

$$Q_{tp,act} = \dot{m}_{ref,cap} \cdot (h_{ref,o} - h_{ref,i})$$ (4.16)

A performance prediction can be performed knowing the inlet states and mass flow rates of the fluids entering the heat exchangers as well as the overall heat transfer area coefficient product of the heat exchanger. Dependent on whether there is sensible heat transfer only or sensible and latent heat transfer, the effectiveness-NTU method for sensible heat exchanger or the analogy approach for wet coils is used for predicting the cooling coil performance.

Table 5.1 Effectiveness-NTU relations for sensible heat exchangers and wet cooling coils

Parameter	Effectiveness-NTU Method for Sensible Heat Exchangers	Effectiveness-NTU Method for Wet Cooling Coils
Effectiveness	$\varepsilon = 1 - \exp(-NTU)$	$\varepsilon = 1 - \exp(-NTU^*)$
Number of transfer units	$NTU = \dfrac{UA}{\dot{C}_{min}}$	$NTU^* = \dfrac{U^* A}{\dot{m}_a}$
Capacitance ratio	$\dot{C}_r = \dfrac{\dot{C}_{min}}{\dot{C}_{max}}$	$m^* = \dfrac{\dot{m}_a}{\dot{m}_{ref}.(C_{p,ref} / C_{p,s})}$
Maximum heat flow	$Q_{max} = \dot{C}_{min}.(T_{h,i} - T_{c,i})$	$Q_{max} = \dot{m}_a.(h_{a,i} - h_{a,sat,ref})$
Actual Heat flow	$Q_{act} = \varepsilon.Q_{max}$ $Q_{act} = \dot{m}.C_{p,h}.(\lvert T_{h,i} - T_{h,o} \rvert)$ $Q_{act} = \dot{m}.C_{p,c}.(\lvert T_{c,i} - T_{c,o} \rvert)$	$Q_{act} = \varepsilon.Q_{max}$ $Q_{act} = \dot{m}_a.(h_{a,i} - h_{a,o})$ $Q_{act} = \dot{m}_{ref}.(h_{ref,o} - h_{ref,i})$

Condensation will occur if the coil surface temperature is below the dew point temperature of the air entering the evaporator. Consequently, there are two cases to consider; either the coil surface is partially wet or it is totally wet. In the case of a partially wet coil, the heat exchanger could be treated as a sensible heat exchanger up to the point where the coil surface temperature equals the dew point temperature. From then on, the coil is treated as a wet coil and the wet coil analogy approach is used. However, to determine the point where the coil surface temperature is equal to the dew point temperature requires a detailed analysis. A simpler approach is to treat the coil either as totally dry (effectiveness-NTU method for sensible heat exchangers) or as totally wet coil (effectiveness-NTU method for wet coils). Both methods slightly under predict the actual heat transfer rate. Therefore, the higher heat transfer rate is used as the predicted performance. According to Braun *et. al.* [37], the error associated with this method is generally less than 5 %.

Using the wet coil analogy approach, the U^*A product used in the wet coil analysis is calculated as shown below in equation (4.17). The evaluation of the heat transfer coefficients on the air side and the refrigerant side is done similar to that of the dry cooling coils.

$$U*A = \frac{1}{\dfrac{C_{p,a}}{(\eta_o hA)_a} + \dfrac{C_{p,a,s}}{(hA)_{ref}}} \qquad (4.17)$$

Thus, the enthalpy based overall heat transfer area coefficient product can be calculated if the heat transfer coefficients for the refrigerant side and the air side are known.

Subsequently, the heat exchanger performance can be performed by using the effectiveness- NTU relationships of the analogy approach for wet coils.

Hence, depending on whether the mean surface temperature of the coil is greater or less than the dew point temperature of the outdoor air, either the dry coil or the wet coil approach will be applied for the cooling coil performance evaluation.

5.4.1 Condenser Modeling Approach

A condenser is a heat exchanger which condenses a substance from its gaseous state to liquid state. In doing so, the latent heat is given up by the refrigerant, and will transfer to the ambient air *i.e.*, condenser coolant. For example, an air conditioner uses a condenser to get rid of heat extracted from the indoor environment to the outside air. Use of surrounding air as the coolant is common in many condensers used in air conditioning applications.

The frontal view of a typical air cooled condenser with fins applied in air conditioning applications is shown in Figure 5.3. Such a condenser can be termed as a compact heat exchanger due to the fact that its heat transfer to volume ratio is relatively high.
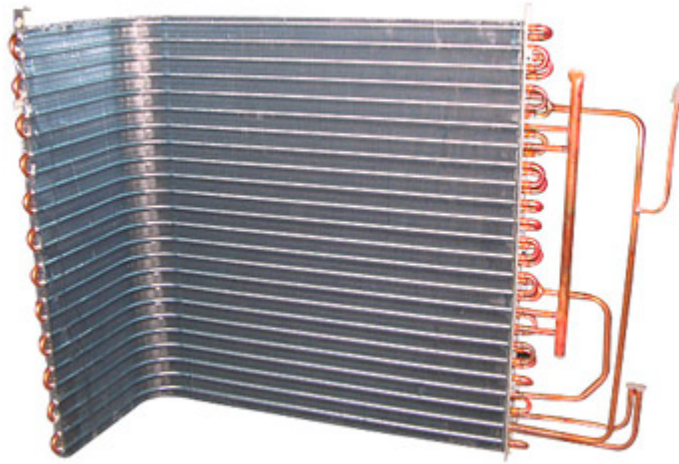
Figure 5.3. Frontal view of a typical air cooled condenser.
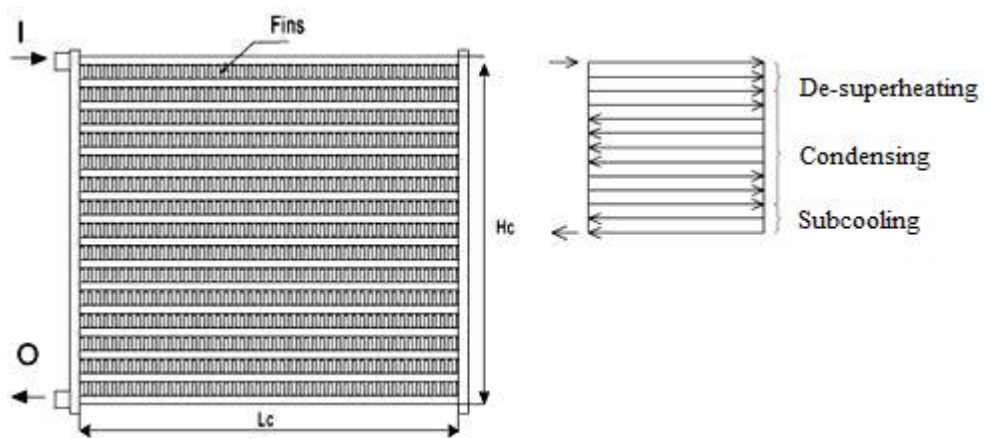
Figure 5.4. Schematic representation of a condenser.

Heat transfer in the condenser is modeled using the effectiveness-NTU method. The condenser heat transfer area is divided into three zones, namely the de-superheating, the two-phase and the sub-cooled zones. Hence, the condenser model consists of a large

number of equations. After leaving the compressor, the refrigerant entering the condenser can be superheated or two-phase. A schematic representation of the condenser is shown in Figure 5.4 where the refrigerant enters the condenser in the form of super-heated vapor at the inlet (*I*) and leaves as liquid refrigerant from the outlet (*O*). The length and the height of the condenser are denoted by L_c and H_c respectively. The sole purpose of the schematic showing the three different zones that normally exists in a condenser is to understand the prevailing heat transfer mechanisms. The modeling strategy of the condenser is classified into these three zones and is presented as follows.

5.4.1. (a) De-superheating Zone

If the condenser inlet refrigerant state is superheated, part of the condenser area is in the de-superheating zone. An iterative method is used to solve equation (4.18) for the number of transfer units (NTU_{dsh}), and the de-superheating area fraction (f_{dsh}) is calculated from equation (4.19). The overall heat transfer coefficient in the de-superheating zone (U_{dsh}) is computed from equation (4.20), while the fin efficiency (η_{fin}) is evaluated from the well-known equation in terms of the fin parameter (*m*) and the airside heat transfer coefficient (h_{as}) as indicated by equation (4.21) and (4.22). The refrigerant side heat transfer coefficient (h_{rs}) is computed from the well-known Dittus–Boelter equation, and the airside heat transfer coefficient (h_{as}) is calculated from the equations proposed by Wang *et. al.* [15-19] based on the fin pattern. The evaluation of the airside heat transfer coefficient based on the Colburn *j*-factor is done using equations (4.24) and (4.25).

$$\varepsilon_{dsh} = \left(1 - exp\left(\left(\left(\frac{NTU_{dsh}^{0.22}}{\dot{C}_c} \right) \cdot \left(exp\left(\left(-\dot{C}_c \cdot NTU_{dsh}^{0.78} \right) \right) - 1 \right) \right) \right) \right) \tag{4.18}$$

$$f_{dsh} = \frac{NTU_{dsh} \cdot \dot{C}_{min,c}}{U_{dsh,c} \cdot A_{cond}} \tag{4.19}$$

$$U_{dsh} = \frac{1}{\left(\dfrac{A_{cond}}{A_{ti,c} \cdot h_{rs,c,dsh}} \right) + \left(\dfrac{1 - \eta_{fin,c}}{h_{as,c} \cdot \left(\left(A_{total,c} / A_{fin,c} \right) + \eta_{fin,c} \right)} \right) + \left(1 / h_{as,c} \right)} \tag{4.20}$$

$$\eta_{fin} = \frac{tanh\left(m \cdot L_c \right)}{m \cdot L_c} \tag{4.21}$$

$$m = \sqrt{\frac{2 \cdot h_{as}}{k \cdot \Delta_{fin}}} \tag{4.22}$$

$$Nu = \frac{h.D}{k_{ref}} \tag{4.23}$$

$$j_c = \frac{Nu}{Re.Pr^{1/3}} \tag{4.24}$$

$$j_c = 0.086 \cdot Re_{D,c,c}^{P_{4,i,c}} \cdot a_c^{P_{5,i,c}} \cdot \left(\frac{P_{f,c}}{D_{c,c}} \right)^{P_{6,i,c}} \cdot \left(\frac{P_{f,c}}{D_{h,c}} \right)^{P_{7,i,c}} \cdot \left(\frac{P_{f,c}}{P_{T,c}} \right)^{-0.93} \tag{4.25}$$

$$\varepsilon_{dsh} = \frac{\dot{C}_{ref,c} \cdot (T_4 - T_5)}{\dot{C}_{min,c} \cdot (T_4 - T_{air,in})} \qquad (4.26)$$

The heat transfer rate of the de-superheating section (q_{dsh}) and the air temperature at the de-superheating zone exit, which is equal to the air temperature at the two-phase zone inlet (T_{atpi}), are calculated from equations (4.27) and (4.28).

$$q_{dsh} = \dot{C}_{ref,c} \cdot (T_4 - T_5) \qquad (4.27)$$

$$T_{atpi,c} = T_{aci} + \left(\frac{q_{dsh,c}}{\dot{C}_{a,c}} \right) \qquad (4.28)$$

5.4.1. (b) Two-Phase Zone

The evaluation method is the same as that in the de-superheating zone, but the refrigerant side condensation heat transfer coefficient in the two-phase region is evaluated from the equation proposed by Traviss *et. al.* [39]. The expression for the effectiveness of a heat exchanger which involves phase change is given by equation (4.29). We know that by definition effectiveness is ratio of the actual heat transfer to the maximum possible heat transfer. Hence, taking '*log$_e$*' on both sides of the equation (4.29) and substituting the equations (4.30) and (4.31). The two-phase area fraction can then be calculated using equation (4.32).

$$\varepsilon = 1 - \exp(-NTU) \tag{4.29}$$

$$\varepsilon = \frac{\dot{Q}_{act}}{\dot{Q}_{max}} = \frac{\dot{C}_a . \Delta T_a}{\dot{C}_{min} . \Delta T_{max}} = \frac{\dot{C}_{ref} . \Delta T_{ref}}{\dot{C}_{min} . \Delta T_{max}} \tag{4.30}$$

$$NTU = \frac{UA_{tot}}{\dot{C}} \tag{4.31}$$

$$f_{tp} = \left(\frac{\dot{C}_{ref,c}}{U_{tp} \cdot A_{cond}} \right) \cdot ln \left(\frac{\dot{C}_{a,c} \left(T_{atpo,c} - T_{atpi,c} \right)}{\dot{C}_{min,c} \left(T_c - T_{atpi,c} \right)} \right) \tag{4.32}$$

Calculation of f_{tp} by equation (4.32) requires $T_{atpo,c}$ which is calculated from equation (4.33).

$$T_{atpo,c} = T_{atpi,c} + \left(\frac{q_{tp}}{\dot{C}_{a,c}} \right) \tag{4.33}$$

It must be noted that this equation is for the refrigerant entering the two-phase section as saturated vapor and leaving as saturated liquid. The heat transfer rate for the two-phase section is readily calculated using equation (4.34).

$$q_{tp} = \dot{m}_{ref} \cdot h_{fg} \tag{4.34}$$

The sub-cooled zone may exist in the condenser, and the sub-cooled fraction (f_{sc}) is calculated from equation below.

$$f_{sc} = 1 - \left(f_{dsh} - f_{tp} \right) \text{ If, } f_{dsh} + f_{tp} \le 1$$

Or

$$f_{sc} = 0 \text{ If, } f_{dsh} + f_{tp} > 1$$

If the sub cooled zone does not exist, i.e. $f_{sc} = 0$, the two phase fraction must be determined from equation (4.35).

$$f_{tp} = 1 - f_{dsh} \tag{4.35}$$

And the heat transfer rate from equation (4.36).

$$q_{tp} = \varepsilon_{tp} \dot{C}_{min} (T_c - T_{atpi,c}) \tag{4.36}$$

Where, the effectiveness of the two-phase zone is given by equation (4.37)

$$\varepsilon_{tp} = 1 - \exp(-NTU_{tp}) \tag{4.37}$$

5.4.1. (c) Sub-cooled Zone

If the sub-cooled fraction is greater than zero, heat transfer for the sub-cooled region in the condenser is evaluated from equations (4.38) through (4.41). The calculation procedure is similar to that of the de-superheating section.

$$NTU_{sc} = \frac{U_{sc} \cdot f_{sc} \cdot A_{cond}}{\dot{C}_{min,c}} \tag{4.38}$$

$$U_{sc} = \cfrac{1}{\left(\cfrac{A_{cond}}{A_{ti,c} \cdot h_{rs,c,sc}}\right) + \left(\cfrac{1 - \eta_{fin,c}}{h_{as,c} \cdot \left(\left(A_{total,c} / A_{fin,c}\right) + \eta_{fin,c}\right)}\right) + \left(1 / h_{as,c}\right)} \tag{4.39}$$

$$\varepsilon_{sc} = 1 - exp\left(\left(NTU_{sc}^{0.22}\right) \cdot \left(exp\left(-\dot{C}_{ref,c} \cdot NTU_{sc}^{0.78}\right) - 1\right)\right) \tag{4.40}$$

$$T_7 = T_c - \left(\varepsilon_{sc} \cdot \dot{C}_{min,c} \cdot \frac{(T_c - T_{atpo,c})}{\dot{C}_{ref,c}}\right) \tag{4.41}$$

It is worth noting that the overall heat transfer coefficient in the sub-cooled zone (U_{sc}) takes the same form as that used to evaluate the overall heat transfer coefficient for the de-superheating zone (U_{dsh}).

The heat transfer rate for the sub-cooled zone can now be calculated from equation (4.42).

$$q_{sc} = \dot{C}_{ref,c} \cdot \left(T_c - T_7\right) \tag{4.42}$$

And the air temperature from the condenser outlet is evaluated from equation (4.43).

$$T_{aco} = T_{aci} + \left(\frac{Q_{cond}}{\dot{C}_{a,c}}\right) \tag{4.43}$$

Where, the total heat transfer rate in the condenser is simply the sum of the heat transfer rates of the three zones given by equation (4.44).

$$Q_{cond} = q_{dsh} + q_{tp} + q_{sc} \tag{4.44}$$

5.5 Pressure Drop in Heat Exchangers

The purpose of the heat exchanger is to transfer thermal energy from one fluid to the other; and for this purpose, it requires fluid pumping power to force the fluid over the heat transfer surface in the exchanger. Hence, pressure drop is considered an important issue in design of a heat exchanger, which must be addressed properly.

The determination of pressure drop (Δp) in a heat exchanger is essential for many applications for at least two reasons. Firstly, the fluid needs to be pumped through the exchanger, which means that fluid pumping power is required. This pumping power is proportional to the exchanger pressure drop. And secondly, the heat transfer rate can be influenced significantly by the saturation temperature change for a condensing or evaporating fluid if there is a large pressure drop associated with the flow. This is because saturation temperature changes with changes in saturation pressure and in turn affects the temperature potential for heat transfer especially for phase change regions.

The pressure drop (Δp) associated with an air-cooled heat exchanger is considered two folds *i.e.* pressure drop in the fin-side or air-side and the pressure drop in the tube-side or refrigerant-side. To overcome the pressure losses incurred when streams flow through heat exchangers, pumps and compressors must be installed. The total cost for a system of pumps and compressors consists of the purchase cost of equipment and the electricity cost to run these equipments. This cost could occupy a significant part of the overall cost for a heat exchanger design. Therefore, the pressure drop aspect should be considered together with the costs for heat exchanger area and utility consumption.

As mentioned earlier the evaluation of the pressure drop is one of the important issues in the designing of the heat exchangers. The pressure drop on the air-side also known as fin-side is estimated using the correlations for the friction factor proposed by Wang *et. al.* [15-19] based on the fin configuration. However, the pressure drop associated with the tube-side or the refrigerant-side of a heat exchanger is considered as a sum of two major contributions: pressure drop associated with the straight tubes, and the pressure drop associated with the return bends. The pressure drop in the tubes can further be classified based on the state of the fluid inside the tubes as, single-phase and two-phase pressure drops. Hence, the pressure drop in the tube-side of a heat exchanger is the sum of the total pressure drop in the straight tube and the return bends as indicated in equation (4.45).

$$\Delta P_{total,HX} = \Delta P_{st,total} + \Delta P_{b,total}$$

(4.45)

Further, the pressure drops in the straight tubes and return bends are the sum of the pressure drops in the individual zones. These zones depend on the phenomenon that takes place in the heat exchanger depending on its application as either a condenser or an evaporator. If the heat exchanger is working as a condenser then three zones may exist in the exchanger namely, de-superheating, two-phase and sub-cooling. However, if the exchanger is working as an evaporator then only two zones exist *i.e.* two-phase and super-heating. A mathematical representation of the pressure drop in a condenser and an evaporator is indicated in equation (4.46) and equation (4.47).

54

$$\Delta P_{tot,cond} = (\Delta P_{st,dsh} + \Delta P_{st,tp} + \Delta P_{st,sc}) + (\Delta P_{b,dsh} + \Delta P_{b,tp} + \Delta P_{b,sc}) \qquad (4.46)$$

$$\Delta P_{tot,evap} = (\Delta P_{st,tp} + \Delta P_{st,sh}) + (\Delta P_{b,tp} + \Delta P_{b,sh}) \qquad (4.47)$$

For evaluating the single-phase pressure drop in straight tubes, the well known expression for the friction factor in terms of the flow Reynolds number and the surface roughness of the tube is used. The friction factor can then be substituted in the well known Darcy-Weisbach equation represented by equation (4.48) to obtain the pressure drop.

$$\Delta P = \rho f (L/D) v^2 / 2g \qquad (4.48)$$

Often the Darcy-Weisbach equation is expressed by equation (4.49).

$$\Delta P = K \rho v^2 / 2g \qquad (4.49)$$

The 'K' in the above equation is known as the total resistance coefficient for the pipeline and is expressed as $K = f(L/D)$. Although the expressions for evaluating the friction factor or in other words the pressure drop, for single-phase *i.e.* de-super heated or super heated or sub-cooled fluid takes the same form, it is in the evaluation of the fluid properties that they differ from each other. Next, the pressure drop in the return bends with single phase can be evaluated using equation (4.49) such that the total resistance coefficient for the return bend (K_B) can be expressed in terms of friction factor in turbulent zone (f_T), radius of the return bend (r), inner diameter of the tube (d), and the

loss coefficient for a 90 degree bend (K) as indicated by equation (4.50). The variable 'n' in the equation (4.50) stands for the number of 90 degree bends in the pipeline. Since, we are working with a return bend $i.e$ 180 degrees the value of n is 2.

$$K_B = (n-1)\left[0.25\pi f_T (r/d) + 0.5K\right] + K \qquad (4.50)$$

The value of the loss coefficient for a 90 degree bend (K) depends on the ratio of the bend radius to the inner diameter of the tube. The 'K' factor as given by Crane Company [24] for the flow of fluids through fittings is illustrated below in Table 5.2 in terms of the friction factor in the turbulent zone (f_T). The turbulent friction factor can be obtained from the well known expression in terms of the flow Reynolds number (Re) and the surface roughness (e).

Table 5.2 'K' factor table

S. No	"r/d" ratio	Loss Coefficient for a 90 degree bend (K)
1.	1	$20\,f_T$
2.	1.5	$14\,f_T$
3.	2	$12\,f_T$
4.	3	$12\,f_T$
5.	4	$14\,f_T$
6.	6	$17\,f_T$
7.	8	$24\,f_T$
8.	10	$30\,f_T$

9.	12	$34\,f_T$
10.	14	$38\,f_T$
11.	16	$42\,f_T$
12.	20	$50\,f_T$

Finally, we are left with the pressure drop in the two-phase state of the refrigerant. The two-phase pressure drop involves the evaluation of the pressure drop in the straight tubes as well as the pressure drop in the return bends. In this regard Pierre [20 and 21] presented a correlation of the two-phase pressure drop in straight tubes based on the tests conducted with R-12 and R-22 refrigerants. The expression for this two-phase pressure drop in straight tubes is given by equation (4.51a).

$$\frac{\Delta P}{L} = \left(f_m + \frac{(x_2 - x_1)D}{x_m L} \right) G^2 \frac{v_m}{D} \qquad (4.51a)$$

Such that x_m and v_m are the mean values of the vapor mass quality and two-phase specific volume respectively.

Further, Pierre was able to correlate the friction factor (f_m) as expressed by equation (4.51b) in terms of the Reynolds number (Re) and the load factor (k_f), provided $R_e / k_f > 1.0$.

.

$$f_m = 0.0185(\text{Re}/k_f)^{0.25} \qquad (4.51\text{b})$$

The load factor is evaluated using equation (4.51c); wherein 'J' is the mechanical equivalent of heat (its value is 778.26 ft-lb$_f$/Btu), h$_{fg}$ is the latent heat of vaporization and Δx is the change in the vapor quality.

$$k_f = J\,\Delta x\,h_{fg}\,/\,L \qquad (4.51\text{c})$$

Due to the success that had been achieved by using the friction factor approach for correlating the two-phase pressure loss in straight tubes, Geary [22] proposed the expression for the two-phase pressure loss in return bends. The pressure drop produced by the return bends is expressed by equations (4.52a), (4.52b), (4.52c) and (4.52d).

$$\Delta P = f\frac{L}{D}\frac{V_g^{\,2}\rho_g}{2g_c} \qquad (4.52\text{a})$$

Such that

$$f = \frac{(5.58E-06)(\text{Re}_g^{\,0.5})}{\exp(0.215C_d\,/\,D)(x^{1.25})} \qquad (4.52\text{b})$$

$$V_g = G\,x\,/\,\rho_g \qquad (4.52\text{c})$$

$$\text{Re}_g = V_g \, D \, \rho_g \, / 12 \mu_g \qquad\qquad (4.52\text{d})$$

CHAPTER 6

EXPANSION DEVICE MODELING

Expansion device is one of the four major components of a vapor compression cycle. It relieves the pressure by a throttling process. Mostly, this throttling process is considered isenthalpic, which means constant enthalpy. Generally, in air conditioning units capillary tubes or thermo-static expansion valves are used. Usually, large systems based on vapor compression refrigeration cycle use a thermo-static valve. While the small systems, make use of a capillary tube as the expansion device.

6.1 Capillary Tube

A capillary tube is a long-length and small-diameter tube, which is used as an expansion device. It controls the refrigerant flow from high-pressure side to low-pressure side in small refrigeration systems. It consists of a long hollow tube with an internal

diameter between 0.51 and 2 mm and a length from 1 to 6 m approximately. Primarily there are two arrangements for the capillary tubes, namely adiabatic and non-adiabatic tubes. The adiabatic capillary tubes expand refrigerant from high pressure to low pressure adiabatically while in the non-adiabatic situation, the capillary tube forms a counter-flow heat exchanger with the suction line that joins the evaporator and the compressor.

6.2 Expansion Valve

An expansion valve is a device used to meter the flow of liquid refrigerant entering the evaporator at a rate that matches the amount of refrigerant being boiled off in the evaporator. Its main purpose like all the other metering devices is to provide a pressure drop in the system, separating the high pressure side of the system from the low pressure side. Thus allowing low pressure refrigerant to absorb heat onto it self.

Expansion valve is considered better than capillary, as it maintains same amount of superheat through out the indoor and outdoor temperature range. As capillary is a simple pipe, the flow rate changes with pressure differential. Therefore, keeping the indoor conditions same, the superheat reduces as the outdoor temperature increases. This is severe in tropical areas. Expansion valve also has a problem. As the superheat is maintained, the discharge temperature is comparatively high at high outdoor temperatures.

6.3 Capillary Tube Modeling Approach

The capillary tube model adopts the equation from American Society of Heating, Refrigerating and Air-Conditioning Engineers (ASHRAE) [41]. In this method, the Buckingham-Pi [29] theorem is applied to the physical factors and fluid properties that affect expansion device flow. The result of this analysis is a group of eight dimensionless Pi terms. The process in the expansion device is assumed adiabatic. The entering state of refrigerant can be sub-cooled or a mixture of liquid and vapor. The effect of coiling the capillary tube is taken into account. This coiling of the capillary tube approximately reduces the refrigerant mass flow rate by 5% when compared with that in a straight tube [42]. Therefore, the eighth dimensionless Pi term is multiplied by 0.95 as shown in equation (5.1). The procedure for determining Π_8 is presented in the correlations proposed by Choi *et. al.* [25].

$$\dot{m}_{ref,cap} = 0.95 \cdot \pi_8 \cdot \left(D_{cap}{}^2\right) \cdot \sqrt{\rho_f \cdot P_{in}} \qquad (5.1)$$

Where π_8 is given by equation (5.2)

$$\pi_8 = 1.313 \times 10^{-3} \cdot \left(\pi_1{}^{-0.087}\right) \cdot \left(\pi_2{}^{0.188}\right) \cdot \left(\pi_3{}^{-0.412}\right) \cdot \left(\pi_4{}^{-0.834}\right) \cdot \left(\pi_5{}^{0.199}\right) \cdot \left(\pi_6{}^{-0.368}\right) \cdot \left(\pi_7{}^{0.992}\right) \quad (5.2)$$

Such that,

$$\pi_1 = \frac{P_{in} - P_{sat}}{P_{crit}} \qquad (5.3)$$

$$\pi_2 = \frac{DSC}{T_{crit}} \qquad (5.4)$$

$$\pi_3 = \frac{L_{cap}}{D_{cap}} \qquad (5.5)$$

$$\pi_4 = \frac{\rho_f}{\rho_g} \qquad (5.6)$$

$$\pi_5 = \frac{\mu_f - \mu_g}{\mu_g} \qquad (5.7)$$

$$\pi_6 = \frac{\sigma}{D_{cap} \cdot P_{in}} \qquad (5.8)$$

$$\pi_7 = \frac{\rho_f \cdot h_{fg}}{P_{sat}} \qquad (5.9)$$

All the properties in the Pi terms are evaluated at the refrigerant state at the inlet to the capillary tube. The refrigerant mass flow rate $\dot{m}_{ref,cap}$ is computed by the expansion

device model and compared with the refrigerant mass flow rate $\dot{m}_{ref,comp}$, which is calculated from the compressor model. If they do not agree within an acceptable tolerance, the condenser pressure (P_4) will be changed according to the scheme shown in Figure 7.1, and the refrigerant mass flow rate will be recalculated until the agreement between $\dot{m}_{ref,cap}$ and $\dot{m}_{ref,comp}$ is established.

The pressure drop in the capillary tube is calculated using the Churchill equation [26], which is used to evaluate the friction factor. The expression is given by equation (5.10).

$$f = 8 \cdot \left(\left((8/Re)^{12} \right) + \left(\frac{1}{(A+B)^{1.5}} \right) \right)^{1/12} \tag{5.10}$$

Where,

$$A = \left(2.457 \cdot ln \left(\frac{1}{\left(\left(\frac{7}{Re} \right)^{0.9} \right) + \left(0.27 \cdot \frac{e}{D_{cap}} \right) \right)} \right) \right)^{16} \tag{5.11}$$

$$B = \left(\frac{37530}{Re} \right)^{16} \tag{5.12}$$

6.4 Expansion Valve Modeling Approach

The expansion device model described here requires a dimensionless correlation to predict refrigerant mass flow rate through the expansion device. A dimensionless

correlation for the mass flow rate has been used to predict the refrigerant mass flow rate for several other expansion devices, but a correlation is seldom seen for an expansion valve in the open literature. The dimensionless parameters given here were selected based on the Buckingham-Pi theorem [29] and generated using the procedures described by Choi *et. al.* [25]. The first step of the theorem was to select the parameters that have an influence on the mass flow rate of refrigerants through the expansion valve.

Because of the sub-cooled inlet conditions, the operating parameters considered are inlet pressure (P_{in}), degree of sub-cooling (ΔT_{sc}), saturation pressure (P_{sat}) corresponding to inlet temperature, outlet pressure (P_{out}), pressure difference (ΔP) and outlet quality (x). The pressure difference (ΔP) is included here because the absolute value of 'ΔP' affects the mass flow rate directly. The thermo-physical property parameters of the refrigerants selected are liquid viscosity (μ_f), liquid density (ρ_f) and surface tension (σ). In addition to these variables, the critical pressure (P_c) and critical temperature (T_c) are also introduced to simplify the correlation. The equivalent diameter (D_e) is selected as the geometry parameter according to the flow area of the valve opening. The value of the equivalent diameter is obtained as manufacturer information that can be found in catalogues.

The correlation for refrigerant mass flow rates through the expansion valve as proposed by Chuan *et. al.* [27] is given by equation (5.13).

$$\dot{m}_{ref,EV} = \pi_9 \cdot \left(D_e^{\,2}\right) \cdot \sqrt{\rho_f \cdot \left(P_{in} - P_{out}\right)} \tag{5.13}$$

Where π_9 is given by equation (5.14).

$$\pi_9 = 19.8529 \cdot \left(\pi_1^{-0.8671}\right) \cdot \left(\pi_2^{0.1312}\right) \cdot \left(\pi_3^{-1.1248}\right) \cdot \left(\pi_4^{-0.5279}\right) \cdot \left(\pi_5^{0.1090}\right) \cdot \left(\pi_6^{0.1820}\right) \cdot$$
$$\left(\pi_7^{-1.3867}\right) \cdot \left(\pi_8^{-0.7304}\right) \tag{5.14}$$

Such that,

$$\pi_1 = \frac{P_{in}}{P_{crit}} \tag{5.15}$$

$$\pi_2 = \frac{P_{out}}{P_{crit}} \tag{5.16}$$

$$\pi_3 = \frac{P_{in} - P_{out}}{P_{crit}} \tag{5.17}$$

$$\pi_4 = \frac{P_{sat}}{P_{crit}} \tag{5.18}$$

$$\pi_5 = \frac{\Delta T_{sc}}{T_{crit}} \tag{5.19}$$

$$\pi_6 = x \tag{5.20}$$

$$\pi_7 = \frac{\sigma}{D_e \cdot P_{in}} \tag{5.21}$$

$$\pi_8 = P_{crit} \cdot \rho_f \cdot \frac{D_e^2}{\mu_f} \tag{5.22}$$

Similar to the capillary tube model, the refrigerant mass flow rate $\dot{m}_{ref,EV}$ is computed by the expansion device model and compared with the refrigerant mass flow rate $\dot{m}_{ref,comp}$, which is calculated from the compressor model. If they do not agree within an acceptable tolerance, P_4 will be changed according to the scheme shown in Figure 7.1, and the refrigerant mass flow rate will be recalculated until the agreement between $\dot{m}_{ref,EV}$ and $\dot{m}_{ref,comp}$ is established.

CHAPTER 7

SYSTEM MODELING

The vapor compression cycle is widely used for air conditioning and refrigeration applications. It is used in small applications such as household refrigerators as well as in large refrigeration applications with a cooling capacity of a couple of hundred kilowatts. Two different kinds of approaches exist for modeling the performance of a whole system such as a vapor compression cycle.

Polynomial expressions are used for the prediction of the total capacity of a vapor compression cycle. The performance of a vapor compression cycle, however, is a function of four input parameters at least, since the performance depends on the entering air's dry bulb temperature, the wet bulb temperature, the volumetric flow rate on the evaporator side and the ambient temperature. Thus, these polynomial expressions contain many curve fit parameters that have to be determined. Stoecker [34] presented

polynomial expressions for the capacity and power requirement of a centrifugal chiller, where 18 coefficients have to be determined in order to predict the system's performance.

Consequently, methods for modeling primary system equipments such as the condenser, the evaporator and the expansion device, are used that are based on fundamental physical principals rather than on polynomial expressions. In these cases, the system is modeled by using empirical or semi-empirical models as presented for the single components in Chapter 3 to Chapter 5. These component models are then matched according to the system layout. The details of the vapor compression cycle are presented in Chapter 1.

7.1 System Modeling Approach

For modeling the system, the component models described in Chapters 4, 5, and 6 are used for the vapor compression cycle model. The models have to describe the performance of each component used in the air conditioning unit in order to predict the overall performance of the system. The compressor type is usually given and compressor performance data can be obtained. Thus, the coefficients of the compressor model can be obtained by fitting the compressor model to the compressor performance data. Having determined these coefficients the compressor model is available for calculation of the thermodynamic state points of the vapor compression cycle.

The mathematical model is coded into a computer program using Engineering Equation Solver (*EES*). This simulation program can be used to calculate parameters of prime interest such as the condenser exit air temperature, the evaporator exit air temperature,

69

the refrigerant mass flow rate, the heat rejection in the condenser and the cooling capacity of the system. All dimensions of the system components such as fin and tube geometry of the evaporator and the condenser, and the dimensions of the expansion device are included in the program. The input data of the program are the initial entering air temperatures of both indoor and outdoor, and the degrees of superheat of the refrigerant at the evaporator exit or inlet to the compressor.

To begin simulation, the program reads the first set of operating condition data, i.e. the air dry bulb and wet bulb temperatures at the evaporator inlet and the air dry bulb and wet bulb temperatures at the condenser inlet whereas the saturated suction temperature (T_e) is assumed. The suction line model is used to determine the state 3, based in the degree of superheat at the compressor inlet. Then the compressor subroutine is used to calculate the compressor power drawn (P_{comp}), the refrigerant mass flow rate ($m_{r,comp}$), the compressor capacity (Q_{comp}) and the compressor work in order to achieve the refrigerant state at the exit of the compressor (T_4). The program proceeds according to the flow chart to evaluate refrigerant states 5, 6, and 7 and the heat rejected from the condenser using the condenser subroutine. Then, the refrigerant mass flow rate ($m_{r,cap}$) is computed by the expansion device model and compared with the refrigerant mass flow rate ($m_{r,comp}$), which is calculated from the compressor model. If they do not agree within an acceptable tolerance, (P_4) will be changed according to the scheme shown in Figure 7.1, and the refrigerant mass flow rate will be recalculated until the agreement between $m_{r,cap}$ and $m_{r,comp}$ is established. This matches the lines that are coming from the compressor to the condenser and the expansion device.

The program then proceeds further according to the flow chart to the evaporator subroutine in order to evaluate refrigerant states 1 and 2, cooling capacity of the evaporator coil considering the throttling process in the expansion device to remain isenthalpic. Further, the new value of the saturated suction temperature is compared with the initially assumed value. If these values remain within a specified tolerance then the program stops or else the entire process will repeat itself until an agreement between the two values is reached.
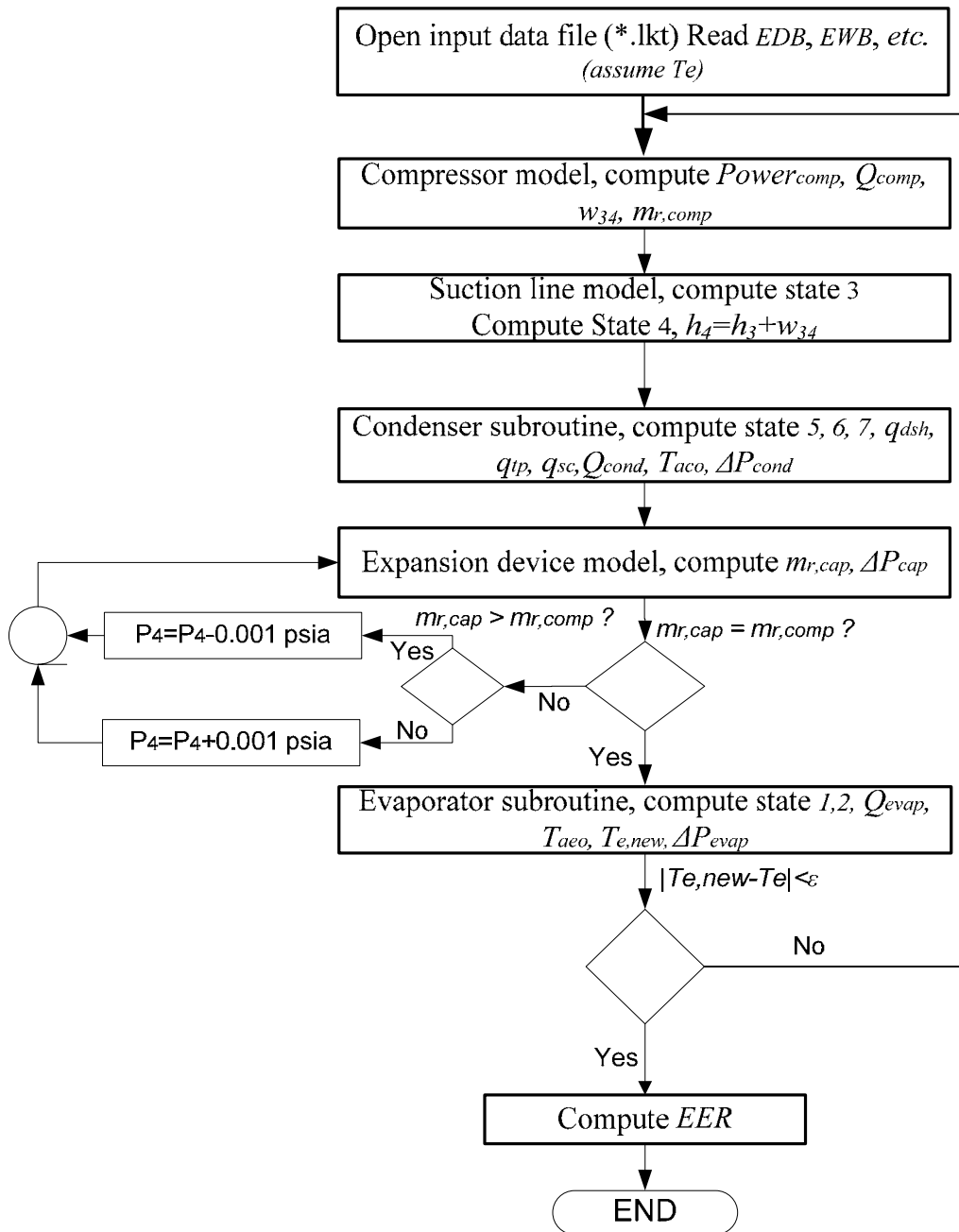
Figure 7.1. Flow chart of the simulation model

At this point, simulation of the model has been finished for the given set of operating condition data. The program can then read another set of operating condition data from the input data file and proceed in a similar manner until the end of the another simulation.

7.2 Model Validation

The mathematical model developed is validated by evaluating the thermal performance of a 10.5 kW air conditioning unit (Unit I). The results obtained from the present code are compared with the experimental results obtained from the manufacturer. Further, these results are also compared with the result obtained from the Oakridge National Laboratories (ORNL) Heat Pump Model. The ORNL heat pump model is a joint development of United States Department of Energy (US DOE) and Oakridge National Laboratories. The DOE/ORNL Heat Pump Design Model is a research tool for use in the steady-state design analysis of air-to-air-heat pumps and air conditioners. The details of the air conditioning 'Unit I' are presented in Table 7.1.

Table 7.1 Details of Air Conditioning Unit I (Package Unit)

Design Variable(s)	Type/Value	
Unit	I	
Test Conditions	ARI Standard	
Compressor model#	CR34KQ-TF5	
Design Variable(s)	Condenser data	Evaporator data
Face area	1.003 sq m (10.8 sq ft)	0.418 sq m (4.5 sq ft)
Tube OD	3.175E-03 m (3/8 inch)	3.175E-03 m (3/8 inch)
Tube wall	0.406E-03 m (0.016 inch)	0.406E-03 m (0.016 inch)
# of horizontal tube rows	1	4
# of vertical tube rows	28	24
Horizontal tube spacing	1.905E-02 m (3/4 inch)	1.905E-02 m (3/4 inch)
Vertical tube spacing	0.025 m (1 inch)	0.025 m (1 inch)
Fin Pitch	16 FPI	14 FPI
Fin thickness	0.139E-03 m (0.0055 inch)	0.139E-03 m (0.0055 inch)
Fan flow rate	3200 CFM	1200 CFM

The validation of the model included the following steps:

1. Curve fitting of the compressor performance data to calculate the coefficients of the compressor model to predict the mass flow rate (C_1-C_{10})

2. Curve fitting of the compressor performance data to calculate the coefficients of the compressor model to predict the compressor power drawn (D_1-D_{10}).

3. Curve fitting of the compressor performance data to calculate the coefficients of the compressor model to predict the compressor capacity (E_1-E_{10}).

4. Using the coefficients that were obtained in steps 1 to 3 in the compressor model to predict the compressor mass flow rate, and the compressor power drawn.

5. Calculation of the thermodynamic state points and rate equations of the vapor compression cycle.

6. Performance evaluation of the condenser model by using the data obtained in step 4.

7. Performance evaluation of the evaporator model by using the data obtained in step 5.

8. Using the data obtained in steps 4-6 in the air conditioning model to predict the total power drawn and the total capacity.

7.2.1 Validation with Experimental Results

The performance of the air conditioning unit predicted using the numerical model is compared with the experimental results obtained from the manufacturer. The manufacturer obtained the experimental results by conducting sample tests in a psychometric testing facility at their location. These facilities maintain the outdoor and indoor test conditions in accordance with the ARI testing standards. The comparison of the results obtained from the present code with those of the experiments conducted by the manufacturer is presented below. Table 7.2 shows the results for air conditioning Unit I (Package Unit).

Table 7.2 Comparison with the Experimental Result

Variable	Experimental	Present Code	% error
EER (Btu/W-h)	7.300	7.385	1.164

It is clear from the results presented in Table 7.2 that the results obtained from the present code are in excellent agreement with the experimental results. However, the difference in the results arises because in the present code, the heat losses from the piping connecting the different components were neglected. In addition, the heat loss from the compressor shell to the surroundings was also neglected. Lastly, the numerical code in the present study makes use of empirical correlations that are fitted based on the experimental results within certain percentage error. Therefore, it is expected that some amount of this error may propagate in the performance prediction using the mathematical modeling.

7.2.2 Validation with DOE/ORNL Heat Pump Design Model (Mark VI) Results

In this section, the performance prediction of the air conditioning unit obtained from the present code is compared with the results obtained from DOE/ORNL Heat Pump model. The DOE/ORNL heat pump simulation program is public domain software (ORNL Mark VI), developed to predict the steady-state performance of vapor compression, electrically driven air-to-air heat pumps.

Table 7.3 Comparison with the DOE/ORNL Heat Pump Design Model (Mark VI) results

Variable	DOE/ORNL Heat Pump	Present Code	% error
EER (Btu/W-h)	7.471	7.385	-1.151

Table 7.3 indicates the results of the performance prediction by the present code are in excellent agreement with that of the DOE/ORNL heat pump model. However, there is a slight variation in the results. This difference in the results arises because the evaluation of the thermodynamic properties in the present code was carried out at the mean temperature of the fluids. Whereas it is not the same in case of DOE/ORNL heat pump model. Since, all the evaluations are done at the backend of the program it is not clear whether it's the mean temperature or the initial temperature.

Further, the effect of the face area while coupled with the volume flow rate on the overall performance of the air conditioning unit is investigated and compared with that of the DOE/ORNL heat pump model.

7.2.3 Effect of face area coupled with the volume flow rate on the AC Performance (Unit I)

In this section we present the results for the effect of the condenser face area coupled with the condenser volume flow rate on the performance of the AC unit. In general when

the effect of any one design variable is studied, all other design variables are kept constant. However, in this case while the effect of the condenser face area on the AC performance is studied, the condenser volume flow rate is also altered. The rate of change of the flow rate with the face area is kept constant, in other words the ratio of the face area to the volume flow rate is kept constant. Hence, with the variation in both the face area and the volume flow rate, the performance of the AC unit is predicted. A comparison of the results obtained from the present code and that of the DOE/ORNL heat pump model is illustrated in the following plots.
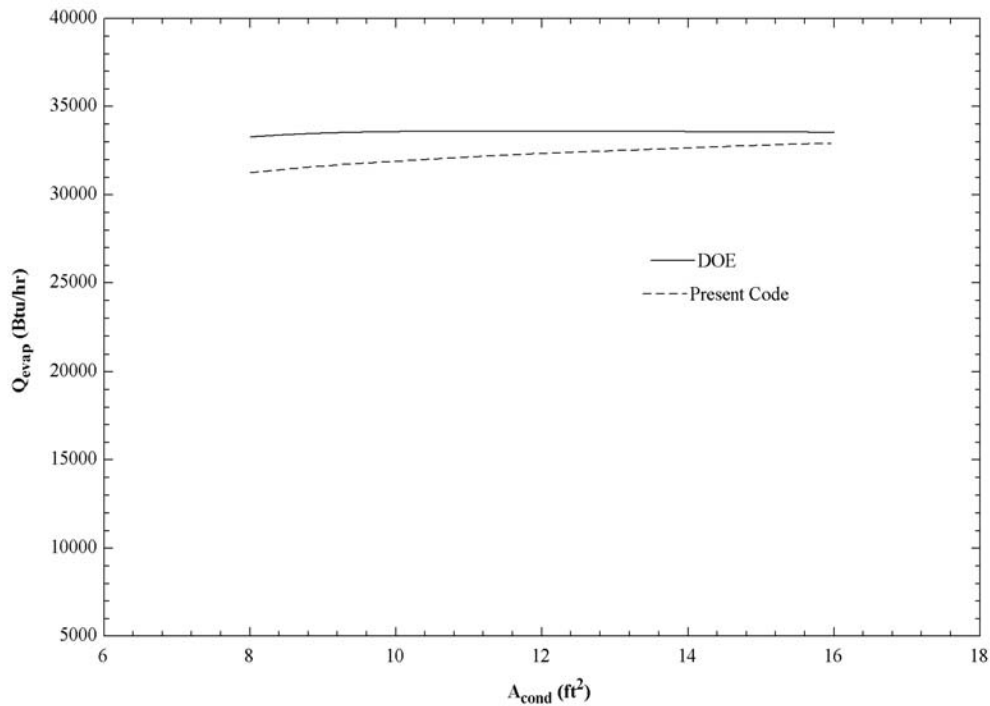

Figure 7.2. Comparison of the effect of condenser face area coupled with volume flow rate on the cooling capacity (Unit I).

Figure 7.2 indicates that with the increase in the condenser face area; there is an increase in the cooling capacity of the air conditioning unit. However, after a substantial increase

in the cooling capacity as a result of the increase in the face area, there is no appreciable increase in the cooling capacity with any further increase in the face area. This phenomenon is represented by the results from both DOE/ORNL heat pump model and the present code.
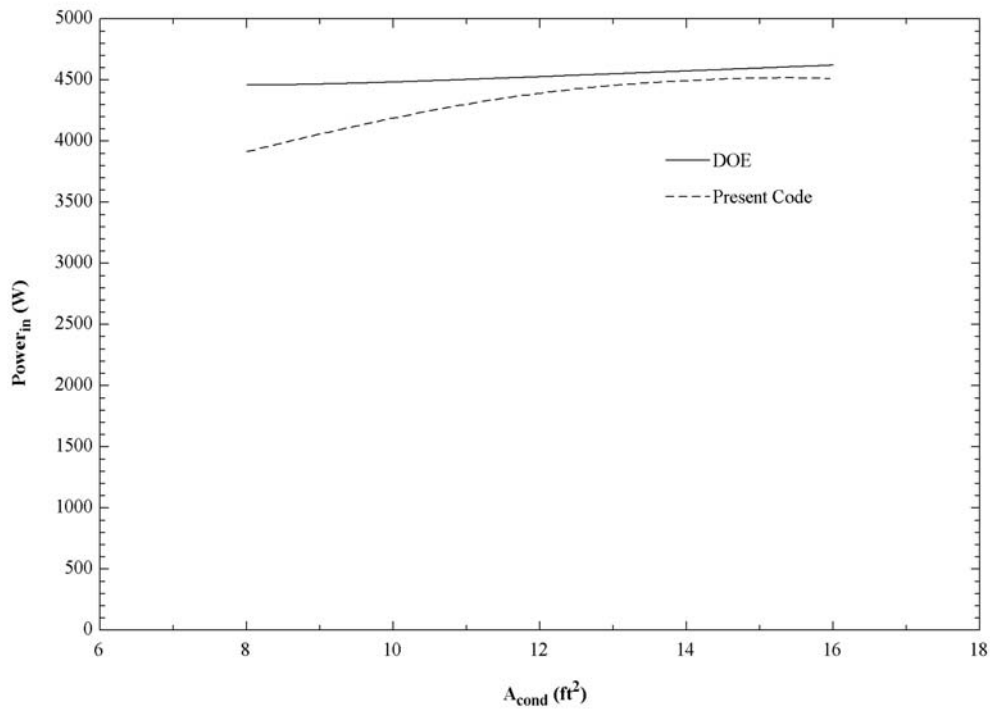

Figure 7.3. Comparison of the effect of the condenser face area coupled with the volume flow rate on the power input (Unit I).

Similarly, Figure 7.3 shows the effect of the condenser face area coupled with the volume flow rate on the power input to the air conditioning unit. The results indicate that both the DOE/ORNL heat pump model and the present code predict the AC performance close enough, near the actual operating conditions. But when the face area is reduced there is a discrepancy. With the decrease in the condenser face area and the volume flow rate there

must be a decrease in the power input. Since, with the decrease in the face area there will be a decrease in the pressure drop in the tube side due to reduced surface area. Also with the decrease in the volume flow rate there will be a decrease in the fan power. On the whole with the decrease in the face area there must be decrease in the power input to the air conditioning unit. This phenomenon is represented by the results obtained from the present code by the dotted line in Figure 7.3. However, in the DOE/ORNL heat pump results, with the decrease in the condenser face area as well as the volume flow rate there is an initial decrease followed by an increase in the power input to the AC unit as indicated.
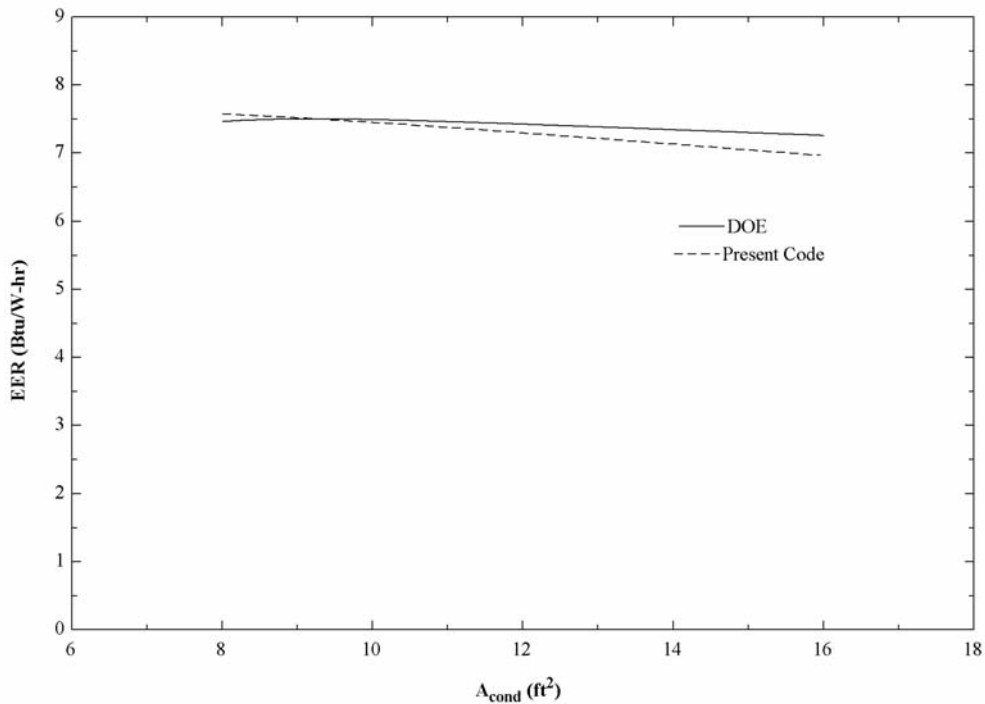

Figure 7.4. Comparison of the effect of the condenser face area coupled with the volume flow rate on the EER (Unit I).

The variation in the results for the effect of condenser face area coupled with the volume flow rate on the power input between the DOE/ORNL heat pump model and the present code affects the impact of the same on the EER. In other words, since EER is nothing but the ratio of the cooling capacity over the power input, the variation in the results of the power input results in the variation in the results for the effect of the condenser face area coupled with the condenser volume flow rate on the unit EER,.

CHAPTER 8

RESULTS AND DISCUSSION

In this chapter we present and discuss the results obtained for the performance prediction of the air conditioning units. We shall also study the different design options modifications that will improve the air conditioning unit's performance. The latter section of this chapter deals with the economic aspects of the suggested design option modifications in the form of cost curves.

Generally, all the air conditioning units are rated at a unified testing conditions recommended by the American Refrigeration Institute (ARI). However, considering the ambient conditions that prevail in the Kingdom of Saudi Arabia, the Saudi Arabian Standards Organization (SASO) recommends testing conditions that are different from ARI. The

Table 8.1 shows the ARI and SASO testing conditions in SI and British units respectively.

Table 8.1 ARI and SASO Testing Conditions

Standard	Outdoor Conditions		Indoor Conditions	
	Dry Bulb Temperature ^{o}C *(F)*	Wet Bulb Temperature ^{o}C *(F)*	Dry Bulb Temperature ^{o}C *(F)*	Wet Bulb Temperature ^{o}C *(F)*
ARI	35 *(95)*	23.9 *(75)*	26.7 *(80)*	19.4 *(67)*
SASO	46 *(114.8)*	24 *(75.2)*	29 *(84.2)*	19 *(66.2)*

The following section presents the results for the air conditioning unit that was mentioned earlier. The effects of different design parameters on the overall performance of the air conditioning unit are also presented.

8.1 Effect of Design variables on the AC Performance
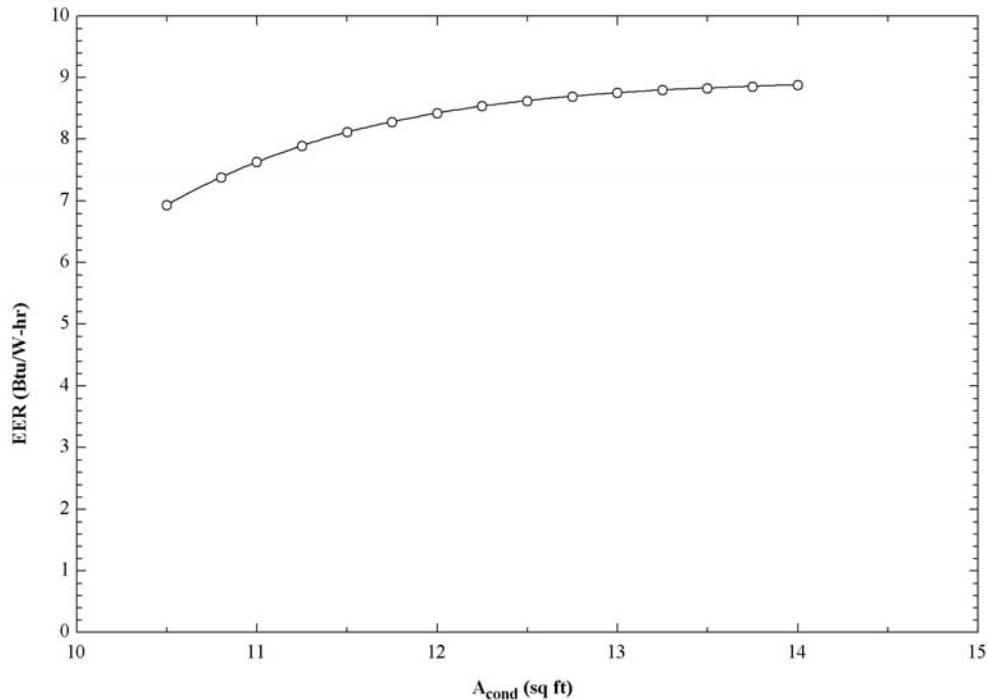
8.1.1 Air Conditioning Unit I (Package Unit)

Figure 8.1. Effect of condenser face area on the AC performance (Package Unit).

Figure 8.1 infers that with an increase in the face area of the condenser the EER of the air conditioning unit increased. This behavior is due to the fact that with an increase in the area there will be an increase in the amount of heat transfer from the given heat exchanger. In addition to this since the above analysis is done at steady state condition it implies that with the increase in the face area of the condenser there will be decrease in the face velocity for a given volume flow rate. This reduction in the face velocity reduces the pressure drop across the exchanger which in turn reduces the power consumption.

Hence, as a result of these two phenomenon's there is an increase in the unit's overall performance with the increase in the condenser face area.
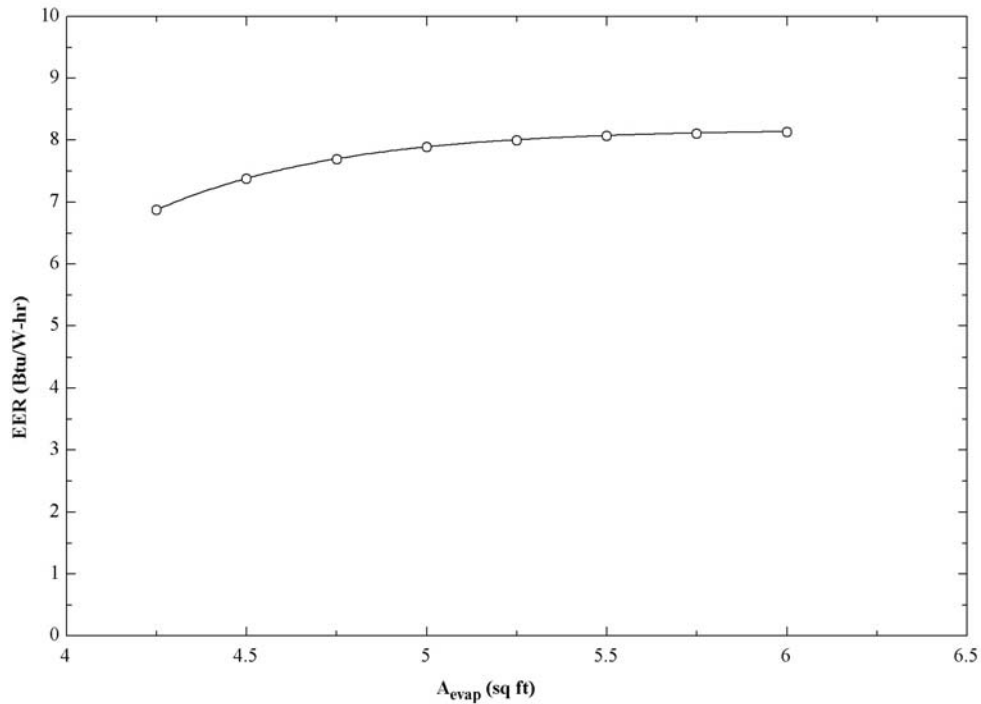

Figure 8.2. Effect of evaporator face area on the AC performance (Package Unit).

Figure 8.2 indicates that, increase in the evaporator face area increased the unit's EER. As explained earlier the increase in the overall performance of the air conditioning unit can be attributed to the increased thermal performance of the exchanger or the reduced power consumption as a result of the reduced pressure drop. Further, if we look carefully the amount of increase in the unit's EER is predominant in the case of variable condenser face area when compared to the evaporator face area for unit I.
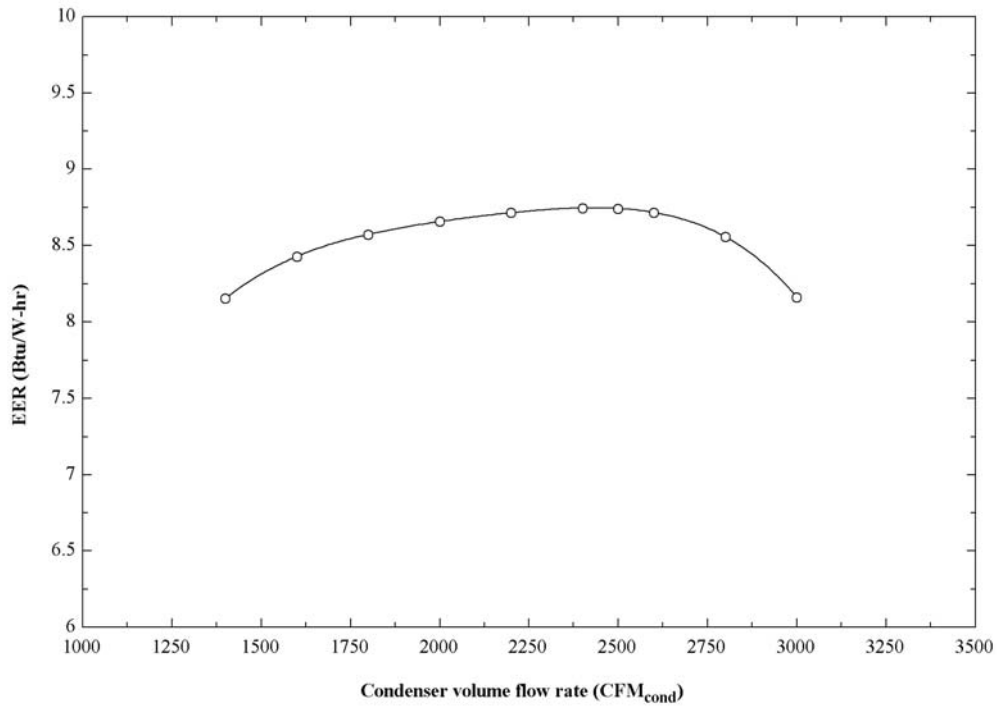
Figure 8.3. Effect of condenser volume flow rate (CFM) on the AC performance (Package Unit).

Figure 8.3 represents the effect of varying the condenser volume flow rate on the overall performance of the air conditioning unit I. The trend from the above figure indicates that with an increase in the condenser air volume flow rate, the overall performance of the unit increases and then decreases. As we already know that with the increase in the volume flow rate there is an increase in the mass flow rate of the fluid. The increase in the mass flow rate of the fluid increases the pressure drop across the heat exchanger and also increases the heat dissipation rate of the condenser. In addition to the increased mass flow rate there is also an increase in the face velocity which increases the friction factor across the exchanger. Since, the pressure drop is directly proportional to the friction

factor; any increase in its value will increase the pressure drop as well as the pumping power. As a result of these opposing effects there exists an optimal value for the volume flow rate of the condenser as indicated in the plot.
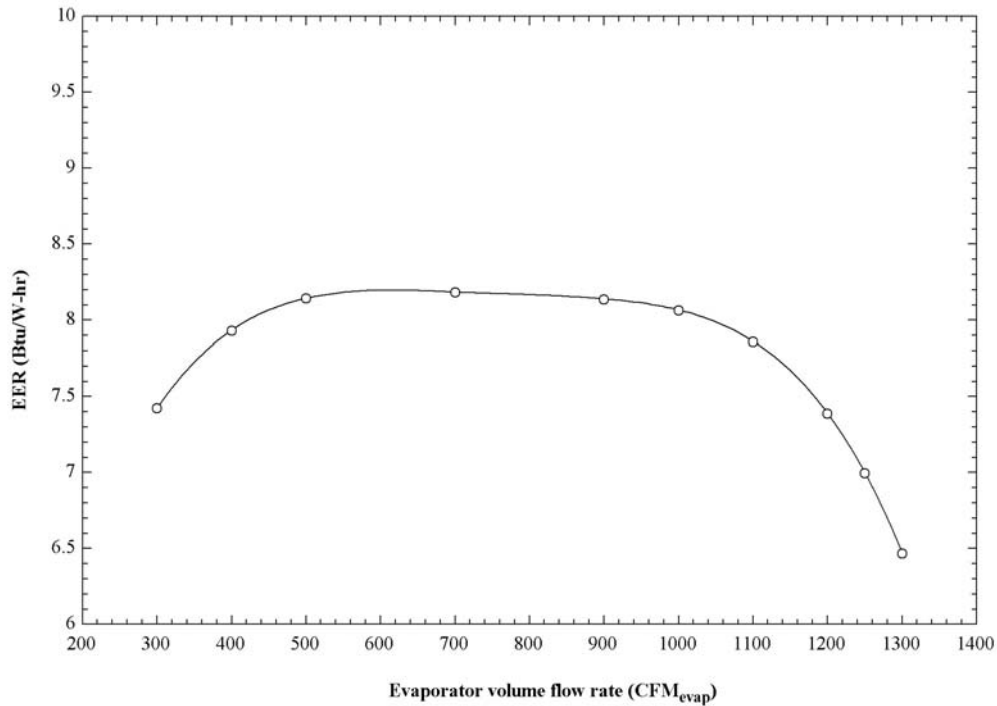

Figure 8.4. Effect of evaporator volume flow rate (CFM) on the AC performance (Package Unit).

Similar to the behavior indicated by the air conditioning unit for the variation in the condenser flow rate there is an increase followed by a decrease in the overall performance of the unit with the increase in the evaporator volume flow rate. In the case of the variable evaporator flow rate we can observe that there is a slight increase in the unit EER followed by a plateau region where the effect of evaporator flow rate is minimal. With further increase in the evaporator flow rate there is a pronounced decrease in the overall performance of the AC unit. Hence, it can be concluded that there exist an

optimal value for the evaporator flow rate where the AC unit yields maximum performance.

The effect of the compressor performance on the overall performance of the air conditioning is presented in the following section. The details of the compressors used are presented in Table 8.2. The rated capacity and the rated EER are obtained based on the test conducted by the manufacturer in accordance with ARI testing standards.

Table 8.2 Compressor Details (Package Unit)

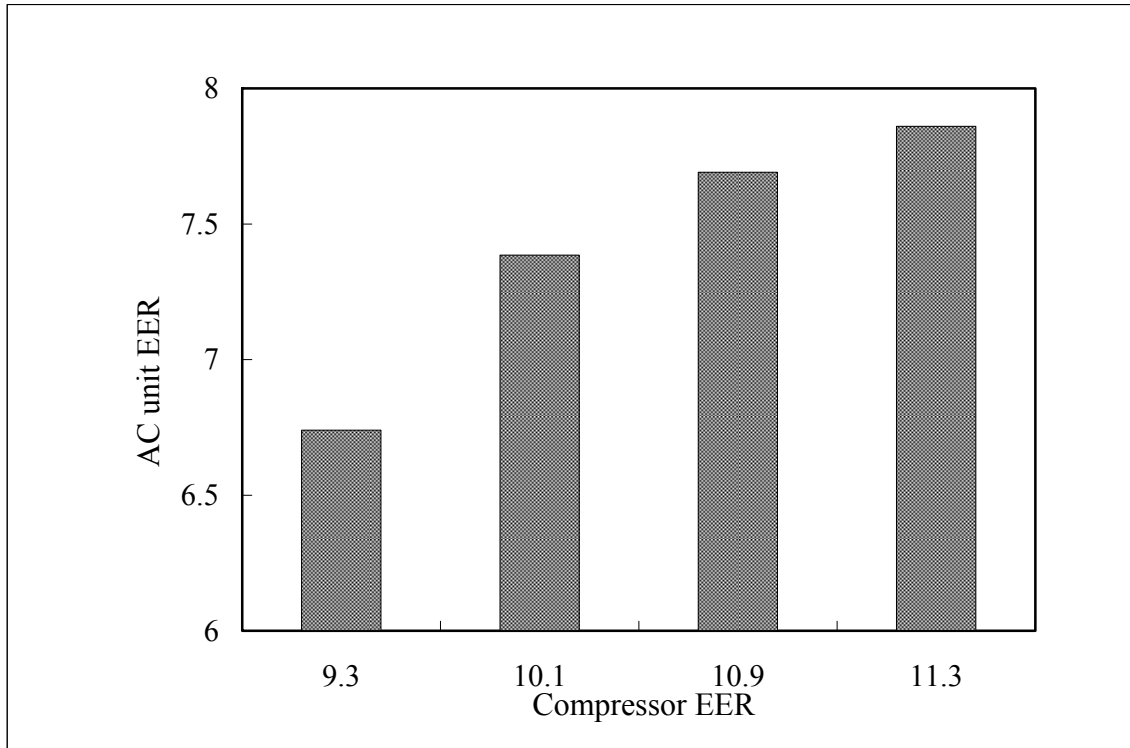| Model#	Rated Capacity (Btu/hr)	Power (W)	Rated EER (Btu/W-hr)
MT040-4	35,777	3,847	9.3
CR34KQ-TF5	33,900	3,356	10.1
CR34K6-PFV	34,500	3,165	10.9
CR35K7-PFV	35,300	3,124	11.3

Figure 8.5. Effect of compressor EER on the AC performance (Package Unit).

The Figure 8.5 indicates that using efficient compressors *i.e.* compressors with high EER, improves the overall performance of the air conditioning unit. It can be inferred that there is a linear relationship between the compressor efficiency (*or compressor EER*) and the overall performance of the air conditioning unit.

8.1.2 Air Conditioning Unit II (Split Unit)

This section presents the results and discussion for the effect of design variables on the overall performance of the air conditioning unit II. The geometry and specifications of the air conditioning unit II are presented in Table 8.3.

Table 8.3 Details of Air Conditioning Unit II (Split Unit)

| Design Variable(s)	Type/Value	
Unit	II	
Test Conditions	ARI Standard	
Compressor model#	AWZ5528	
Design Variable(s)	Condenser data	Evaporator data
Face area	0.511 sq m (5.5 sq ft)	0.299 sq m (3.22 sq ft)
Tube OD	0.008 m (5/16 inch)	0.01 m (3/8 inch)
Tube wall	0.0004 m (0.016 inch)	0.0006 m (0.022 inch)
# of horizontal tube rows	2	3
# of vertical tube rows	26	3
Horizontal tube spacing	0.016 m (5/8 inch)	0.019 m (3/4 inch)
Vertical tube spacing	0.0254 m (1 inch)	0.0254 m (1 inch)
Fin Pitch	16 FPI	12 FPI
Fin thickness	1.143E-04 m (0.0045 inch)	1.143E-04 m (0.0045 inch)
Fan flow rate	1400 CFM	490 CFM
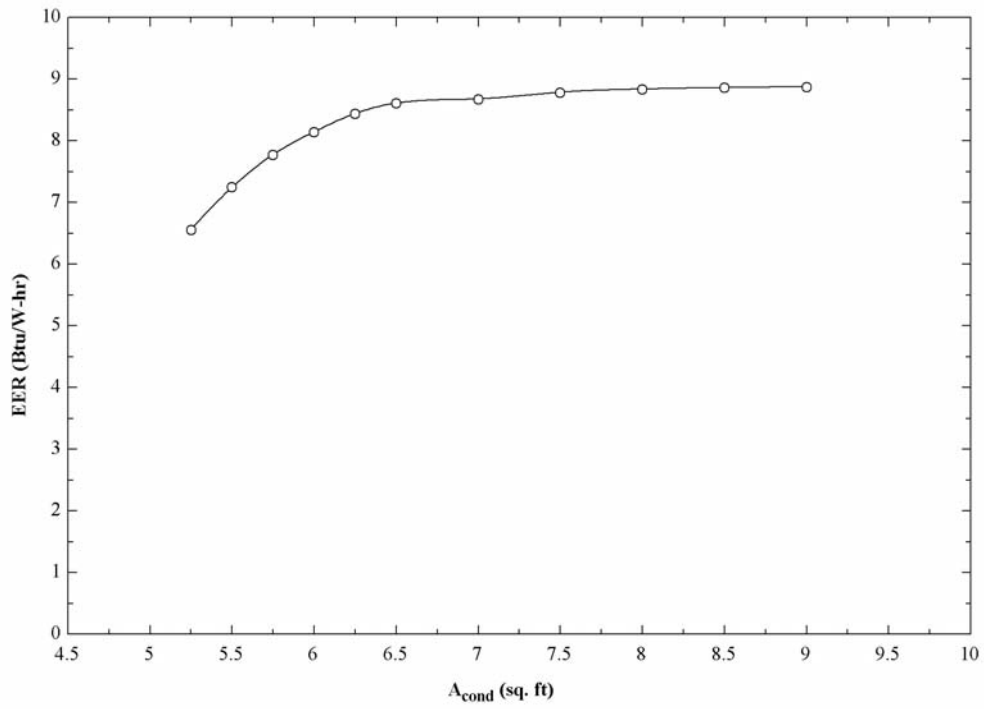
Figure 8.6. Effect of condenser face area on AC performance (Split Unit).
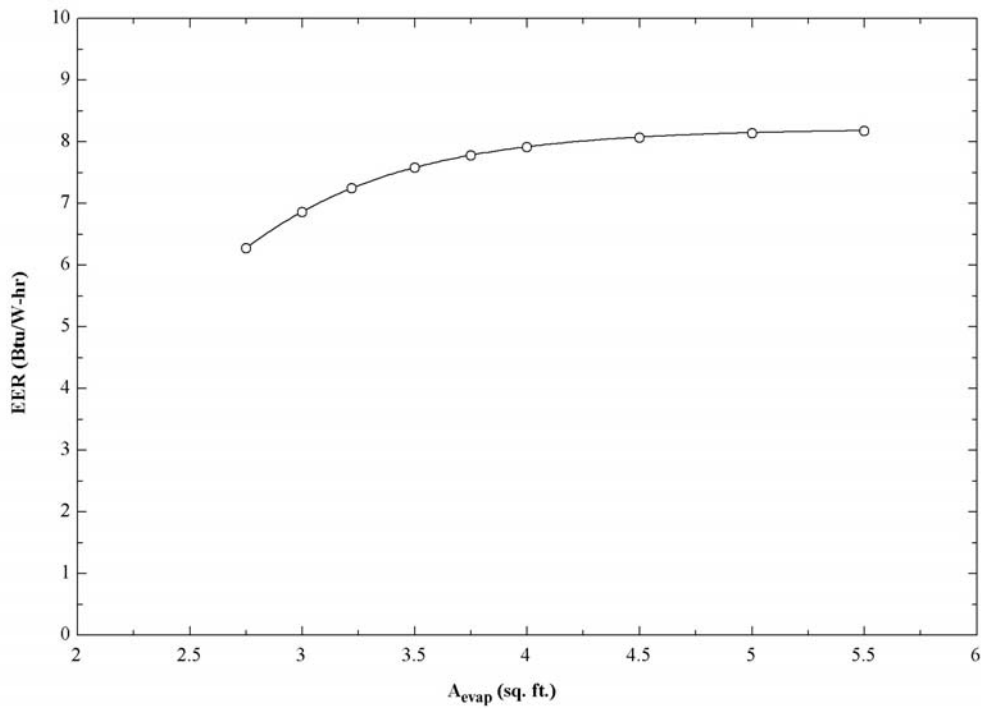
Figure 8.7. Effect of evaporator face area on AC performance (Split Unit).
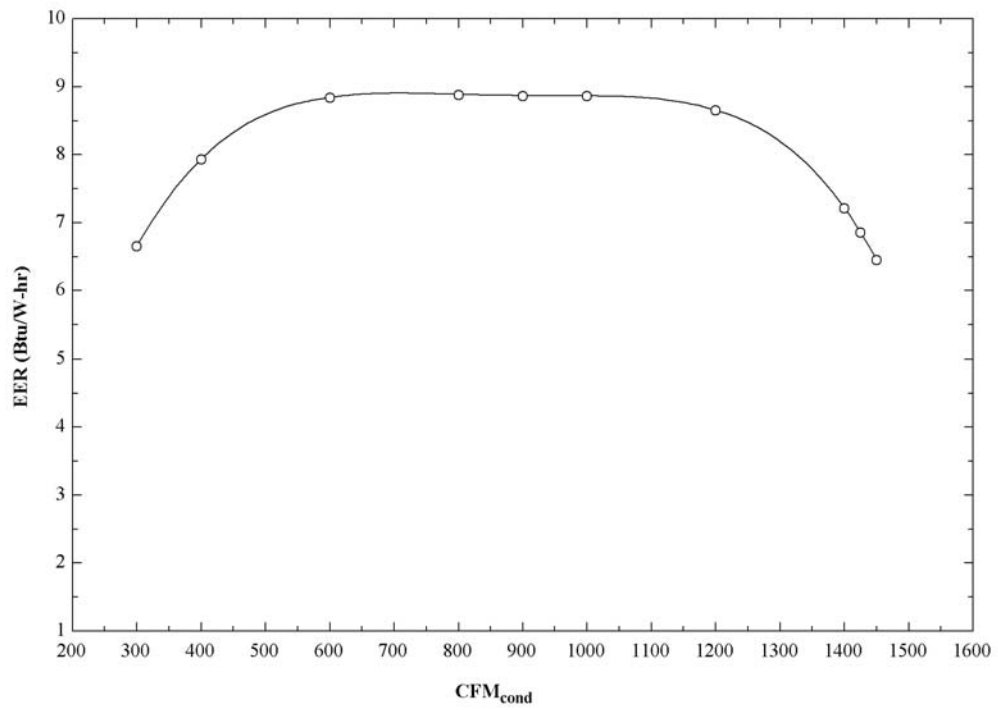
Figure 8.8. Effect of condenser volume flow rate on the AC performance (Split Unit).
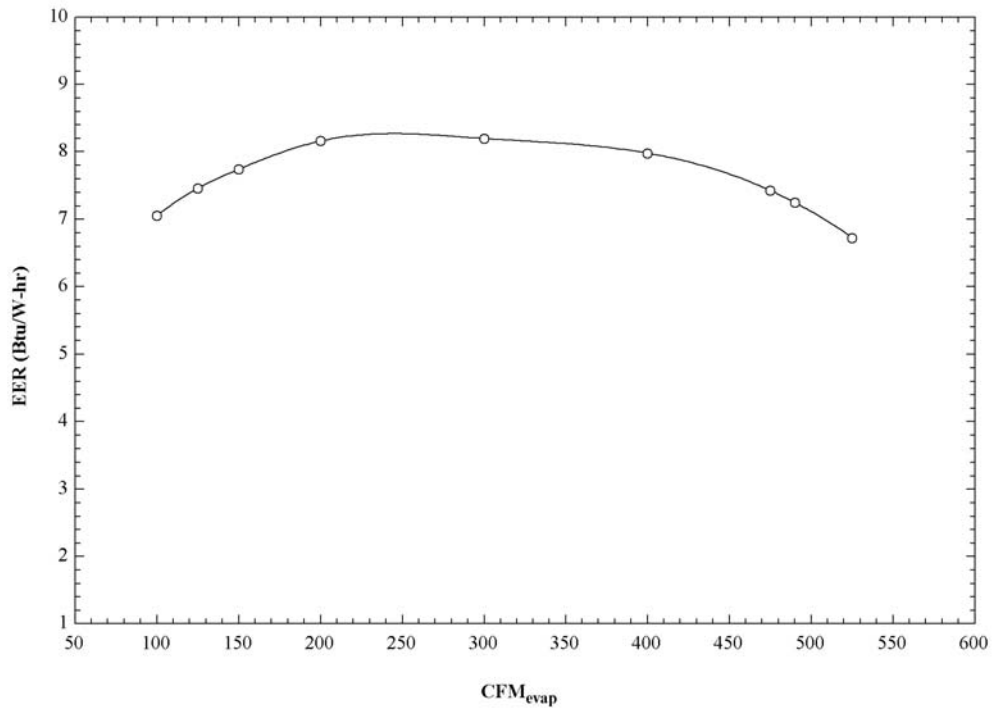
Figure 8.9. Effect of evaporator volume flow rate on the AC performance (Split Unit).

The details of the compressors used in the analysis of the split unit are presented in Table 8.4.

Table 8.4 Compressor Details (Split Unit)

Model#	Rated Capacity (Btu/hr)	Power (W)	Rated EER (Btu/W-hr)
CR30KQ-PFV	24,700	2,600	9.5
CR28KQ-PFZ	23,400	2,294	10.2
CR24K6-PFV	24,500	2,248	10.9
ZR30KS-PFZ	25,000	2,232	11.2
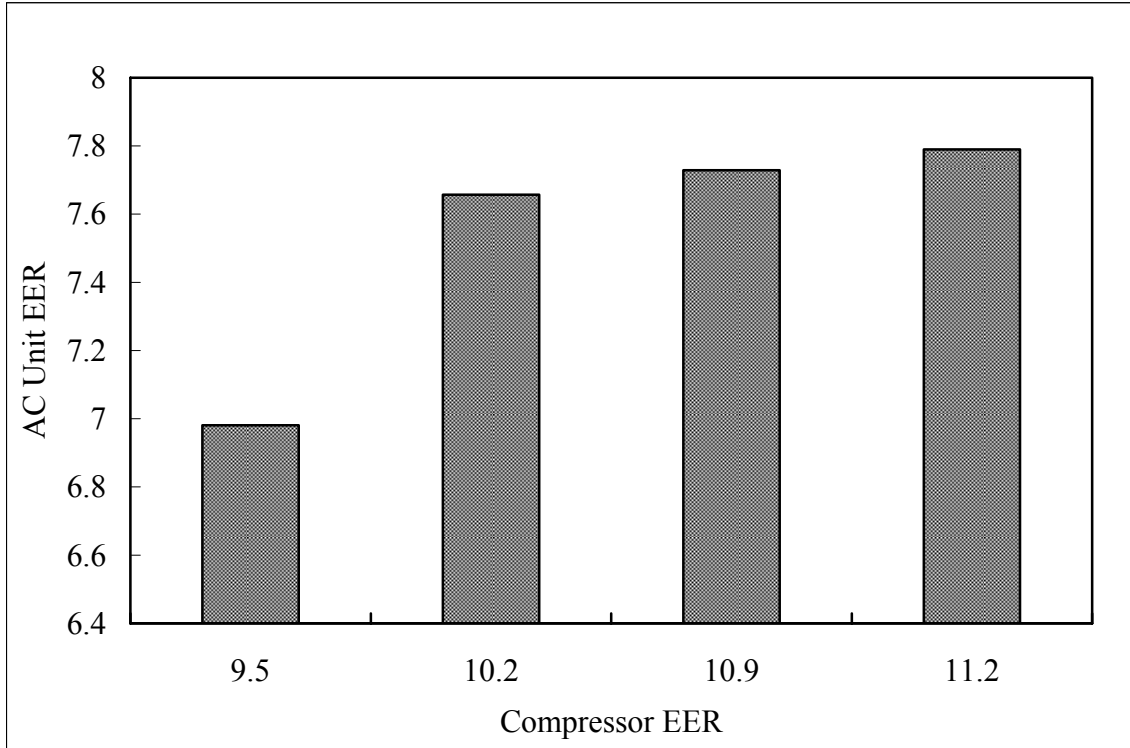
Figure 8.10. Effect of compressor EER on AC performance (Split Unit).

8.1.3 Air Conditioning Unit III (Window Unit)

The following section presents the results and discussion for the effect of design variables on the overall performance of the air conditioning unit III. The geometry and specifications of the air conditioning unit III are presented in Table 8.5.

Table 8.5 Details of Air Conditioning Unit III (Window Unit)

Design Variable(s)	Type/Value	
Unit	III	
Test Conditions	ARI Standard	
Compressor model#	CR140H6B	
Design Variable(s)	Condenser data	Evaporator data
Face area	0.228 sq m (2.45 sq ft)	0.148 sq m (1.59 sq ft)
Tube OD	0.007 m (0.28 inch)	0.008 m (5/16 inch)
Tube wall	0.00027 m (0.011 inch)	0.0004 m (0.016 inch)
# of horizontal tube rows	2	3
# of vertical tube rows	19	15
Horizontal tube spacing	0.0127 m (0.5 inch)	0.016 m (5/8 inch)
Vertical tube spacing	0.021 m (0.83 inch)	0.0254 m (1 inch)
Fin Pitch	16 FPI	14 FPI
Fin thickness	1.143E-04 m (0.0045 inch)	1.143E-04 m (0.0045 inch)
Fan flow rate	390 CFM	320 CFM
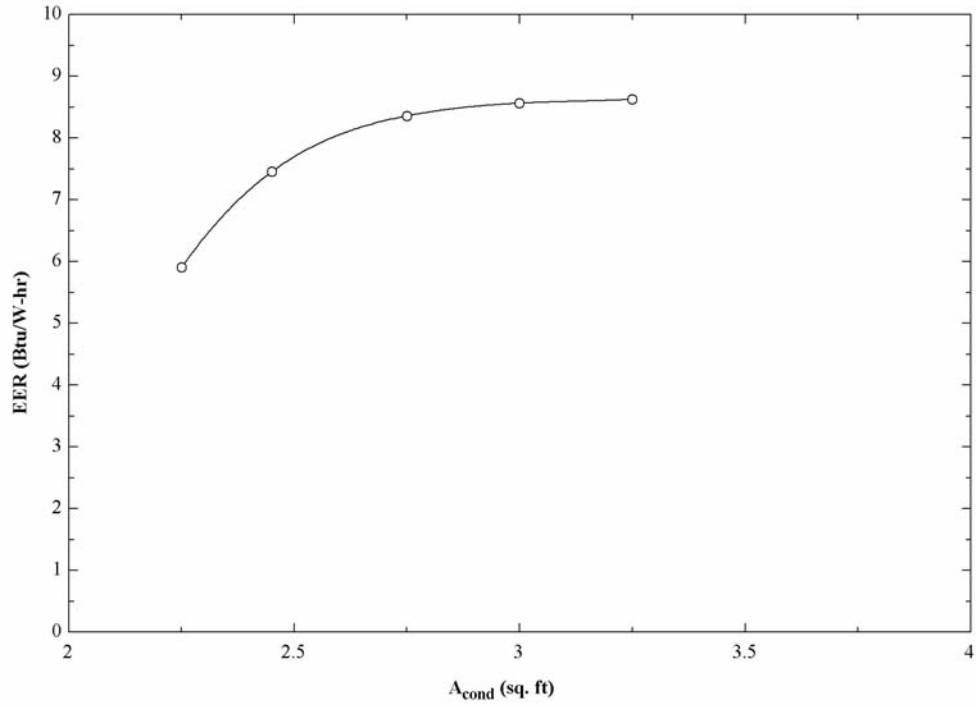
Figure 8.11. Effect of condenser face area on AC performance (Window Unit).
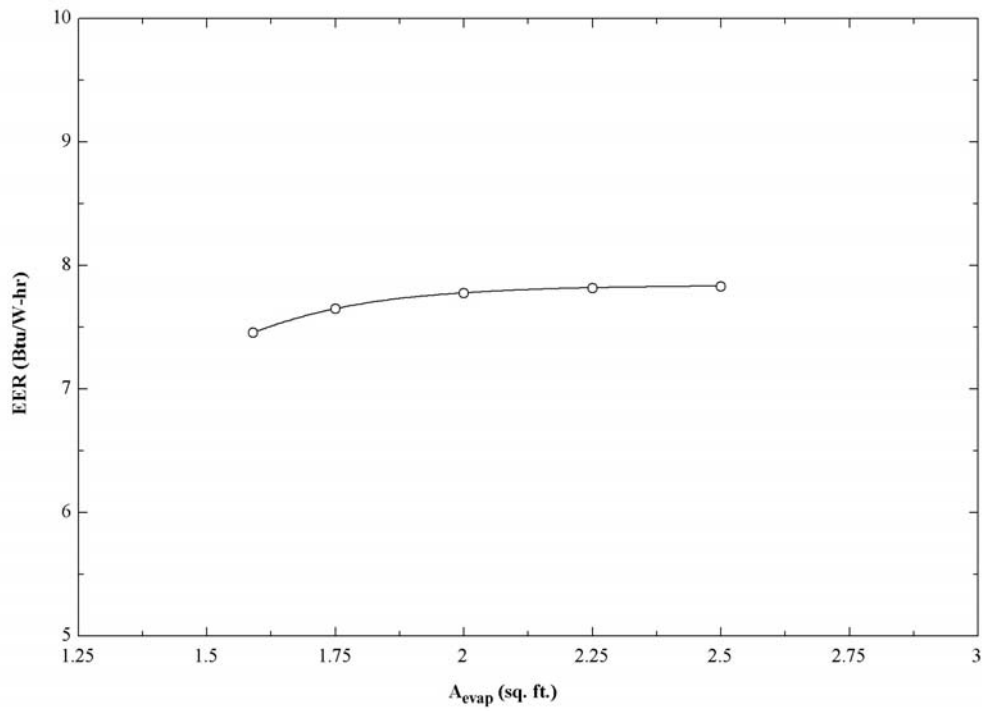
Figure 8.12. Effect of evaporator face area on AC performance (Window Unit).
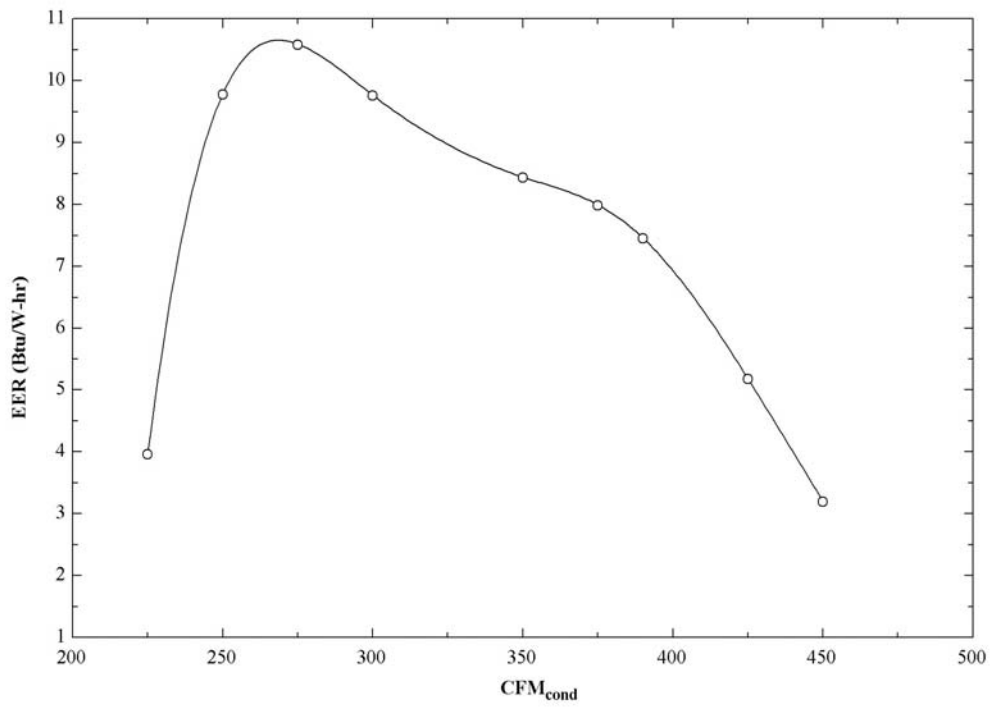
Figure 8.13. Effect of condenser volume flow rate on AC performance (Window Unit).
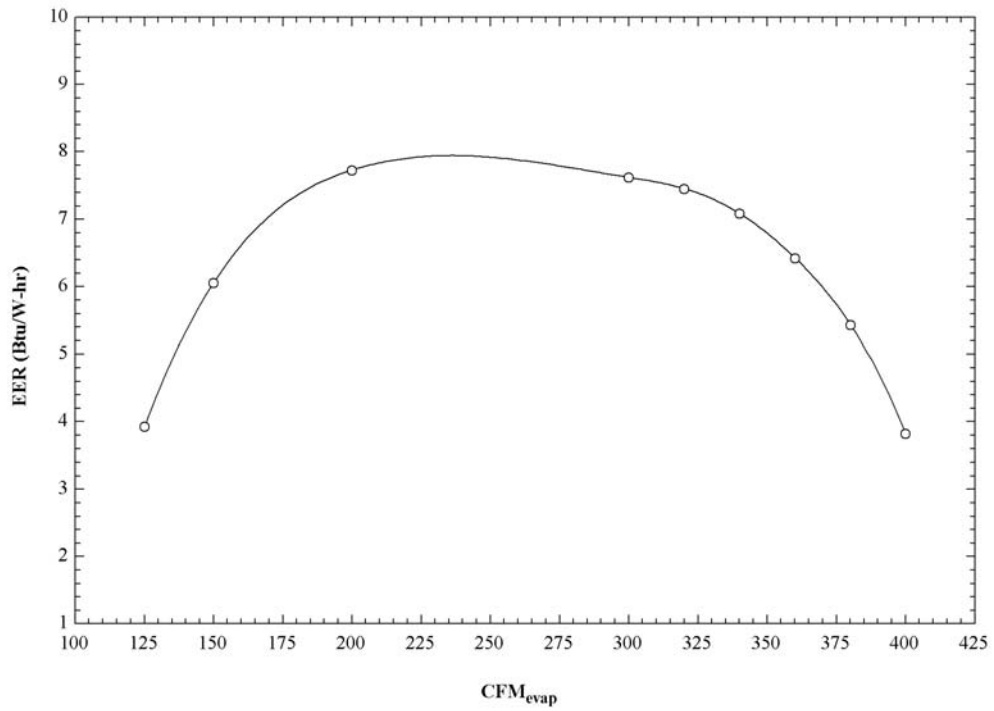
Figure 8.14. Effect of evaporator volume flow rate on AC performance (Window Unit).

The details of the compressors used in the analysis of window unit are presented in Table 8.6.

Table 8.6 Compressor Details (Window Unit)

Model#	Rated Capacity (Btu/hr)	Power (W)	Rated EER (Btu/W-hr)
CR18KQ-PFV	18,400	1,859	9.9
CR20KQ-PFV	19,800	1,980	10
CR18K6-PFV	18,000	1,698	10.6
CR21K7-PFV	21,000	1,927	10.9
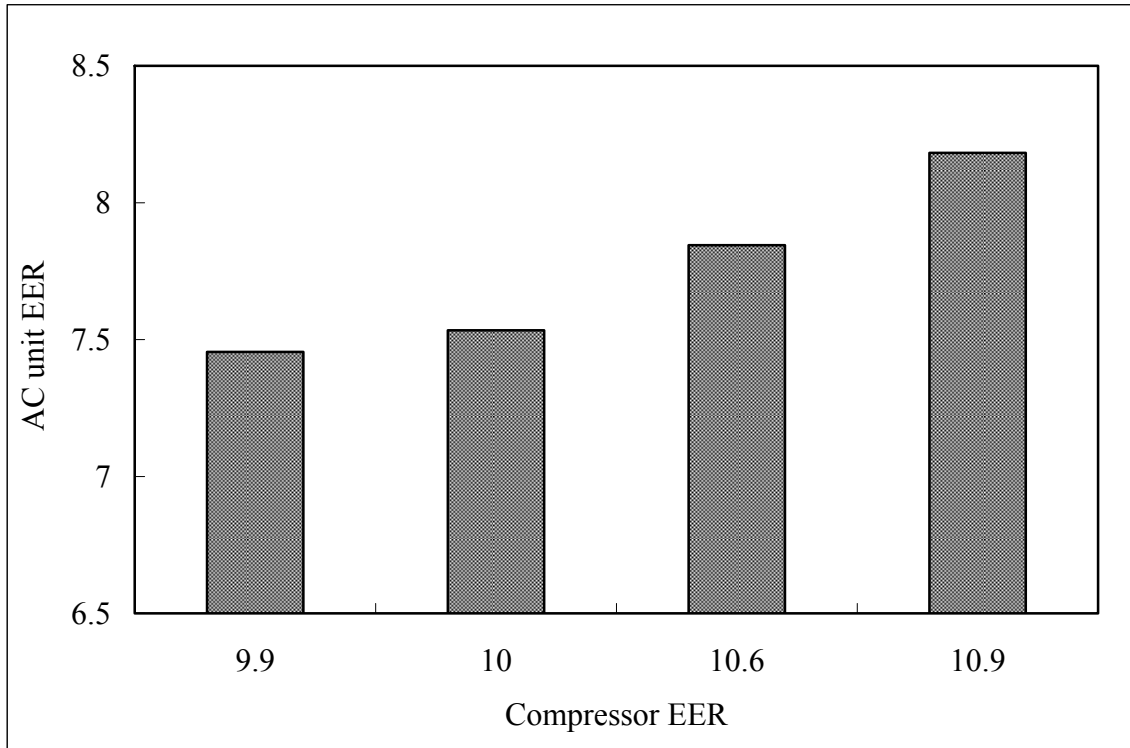
Figure 8.15. Effect of compressor EER on AC performance (Window Unit).

Although, the trends obtained in the above section have a similar behavior for a given design variable; the amount of variation is case specific. Because each air conditioning unit is unique in itself inspite of the similar trends they have to be considered individual entities. Figure 8.1 to Figure 8.4 indicate that there exists an optimal value for the face areas as well as the volume flow rates which can improve the overall performance of an air conditioning unit. However, these optimal values must remain realistic and feasible for the manufacturer considerations.

The design parameters that where studied in the previous section can improve the overall performance of the air conditioning unit. Depending upon the effect that each of these

parameters has on the overall performance of the air conditioning unit they can be considered as the possible design option modifications. The main objective of these design option modifications is to increase the EER of the unit. Sometimes, these design options modifications can independently improve the unit's performance. But mostly they are applied in conjunction with one another. As a result of these conjunctions the performance of the air conditioning unit is enhanced.

8.2 Comparison of AC Performance under Capillary Tube and Expansion Valve

Table 8.7 Comparison of AC Performance under Capillary Tube and Expansion Valve
(Package Unit)

Parameter	Under Capillary Tube	Under Expansion Valve
EER (Btu/W-hr)	7.385	7.815

Table 8.7 compares the AC performance using capillary tube and expansion valve as its expansion device. It can be seen that the AC performance as indicated by the unit EER is better in case of expansion valve as compared to the capillary tube. The slight superior performance of the expansion valve over the capillary tube is because the expansion valve has better control over the refrigerant flow. However, the AC unit can vary in its performance on a case-to-case basis unless; the expansion device is selected properly.

CHAPTER 9

ECONOMIC ANALYSIS

According to the Business Dictionary the definition of economic analysis is as follows:

"Systematic approach to determining the optimum use of scarce resources, involving comparison of two or more alternatives in achieving a specific objective under the given assumptions and constraints. It takes into account the opportunity costs of resources employed and attempts to measure in monetary terms the private and social costs and benefits of a project to the community or economy."

The effect of the design variables presented in the previous sections indicates that these variables can be considered potential design option modifications. The main purpose of these design option modifications is to improve the overall performance of the AC unit.

These design options can be applied either individually or in combination to enhance the performance of the air conditioning unit.

Out of the several design option modifications presented in the previous sections only a select few can be considered as potential enough to provide the desired effect. Hence, Table 9.1 to Table 9.3 shows only those design options that have the potential to improve the overall performance of the air conditioning units with some increase in its cost.

Table 9.1 Design Option Modifications to AC Unit I (Package Unit)

S.no.	Design Modification	% inc in cost	% inc in EER
1	Base line (9.3EER compressor)	-	-
2	1 + 10% increase in condenser face area	1.22	10.29
3	2 + 10% increase in evaporator face area	3.19	17.86
4	3 + 10.1 EER compressor	17.31	30.61
5	3 + 10.9 EER compressor	31.22	37.85
6	3 + 11.3 EER compressor	38.14	41.79

Table 9.2 Design Option Modifications to AC Unit II (Split Unit)

S.no.	Design Modification	% inc in cost	% inc in EER
1	Base line (9.5EER compressor)	-	-
2	1 + 10% increase in condenser face area	3.23	10.90
3	2 + 10% increase in evaporator face area	4.90	16.96
4	3 + 10.2 EER compressor	20.52	31.07
5	3 + 10.9 EER compressor	35.95	32.52

Table 9.3 Design Option Modifications to AC Unit III (Window Unit)

S.no.	Design Modification	% inc in cost	% inc in EER
1	Base line (9.9EER compressor)	-	-
2	1 + 10% increase in condenser face area	3.21	11.04
3	2 + 10% increase in evaporator face area	5.13	14.25
4	3 + 10.0 EER compressor	7.80	15.81
5	3 + 10.6EER compressor	29.86	21.49
6	3 + 10.9 EER compressor	39.94	28.24

Table 9.3 is presented in Figure 9.1 to Figure 9.3 known as the Energy Efficiency-Cost Curves. These curves indicate the increase in the air conditioning unit's EER with the increase in the cost as a result of the modifications in the design.
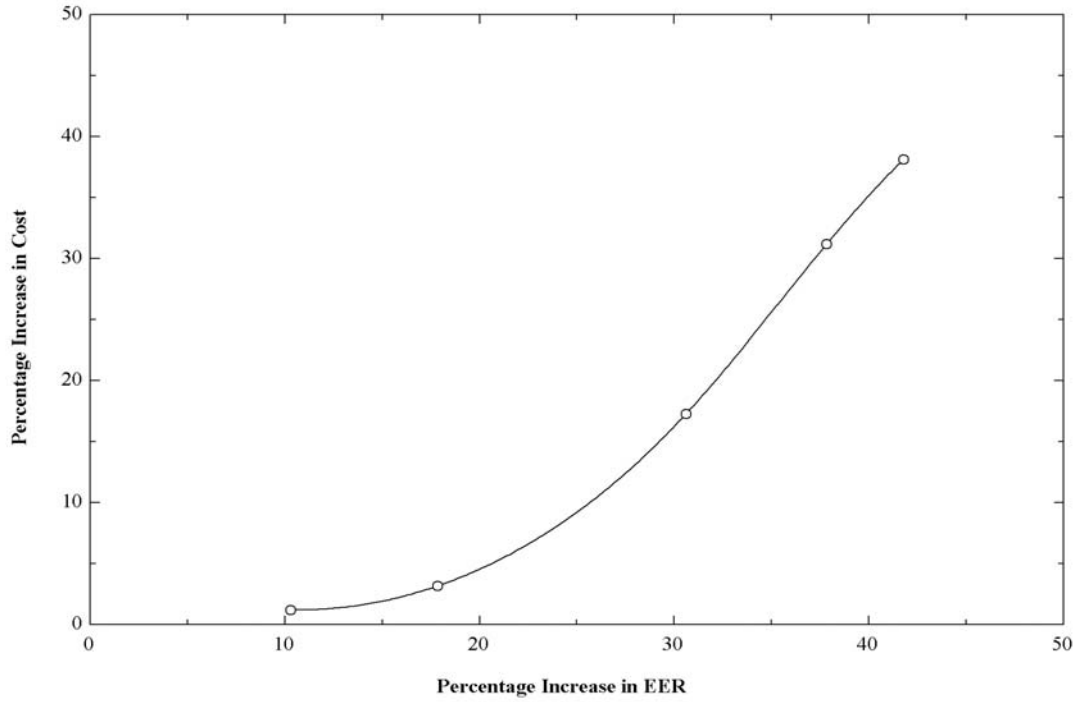
Figure 9.1. Cost curve relating the increase in cost to increase in EER (Package Unit).
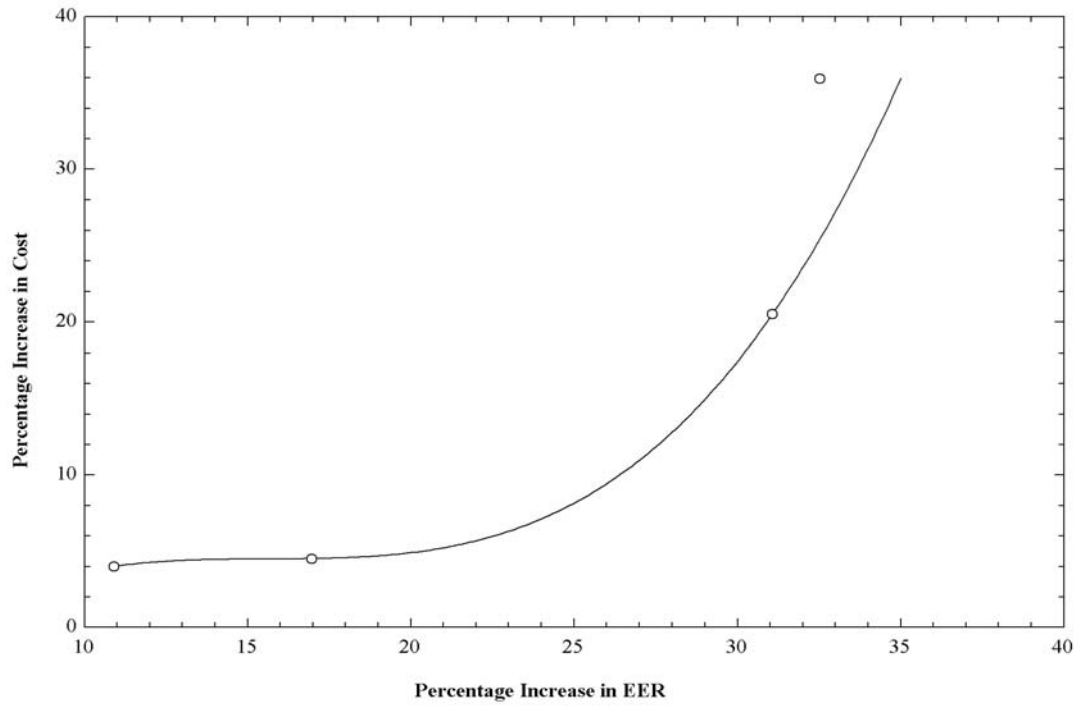
Figure 9.2. Cost Curve relating to increase in cost to increase in EER (Split Unit).
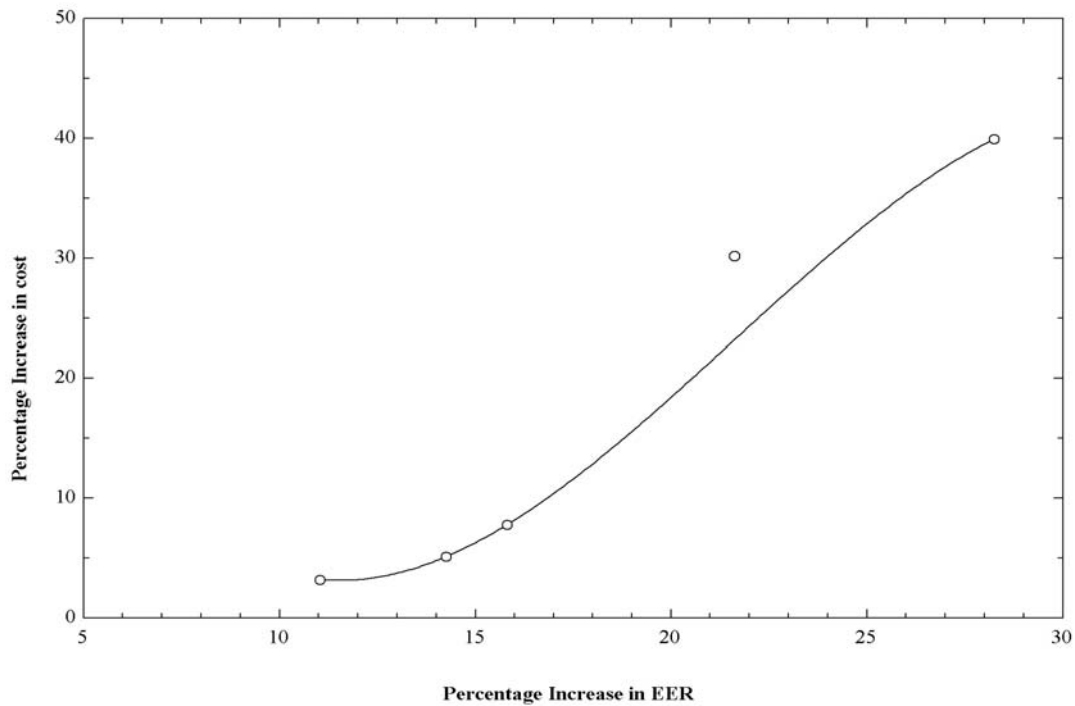
Figure 9.3. Cost Curve relating the increase in cost to increase in EER (Window Unit).

To evaluate the economic feasibility of the proposed design options modification or enhancements, one must take into consideration the manufacturer cost estimates that influence the operating costs. While the life cost analysis which is based on the pay-back-period will be used in analyzing the design options modification from the consumer point of view. The purchasing cost (*PC*), the installation cost (*IC*) and the maintenance cost (*MC*) are the three essential elements for the evaluation of the pay-back-period (*PBP*) of the proposed enhancements. The design option modification is selected based on the evaluated individual pay-back-period. Depending on the extent to which each of the proposed design option modification is effective, they can be selected as an individual alternative or a combination of more than one design option alternatives.

The pay-back-period which is one of the deciding variable can be defined as, the ratio of the sum of the change in the purchasing cost and the installation cost from the baseline unit to the proposed design option to the difference between the change in the operating cost and the manufacturing cost from the baseline unit to the proposed design option. It must be clear that since the modifications are meant to improve the performance of the unit, the purchasing cost, and the installation cost will tend to increase while the operating cost is expected to decrease. The expression to evaluate the pay-back-period is given by Equation 7.1.

$$PBP = \frac{\Delta PC + \Delta IC}{\Delta OC - \Delta MC} \qquad (7.1)$$

However, for purpose of the analysis, one can assume that none of the design options are expected to impact either the installation or the maintenance cost of the equipment. Thus, the pay-back-period can be reduced to the Equation 7.2.

$$PBP = \frac{\Delta PC}{\Delta OC} \qquad (7.2)$$

The change in the purchasing cost (ΔPC) of the equipment can be expressed as the increase in the manufacturing most (*MFC*) as a result of the proposed design option modification over the baseline unit, multiplied by the manufacturer to retail price mark-up (*MU*). It can be expressed according to the Equation 7.3.

$$\Delta PC = (MFC_{design\,option} \ - \ MFC_{baseline\,unit}).MU \qquad (7.3)$$

Similarly, the change in the operating cost (ΔOC) of the equipment can also be expressed as the decrease in the annual energy consumption (*AEC*) as a result of the proposed design option modification over the baseline unit, multiplied by the average electricity price (*EP*) in Saudi Riyal per kilo-Watt hour (*SAR/kWh*). The expression representing the change in the operating cost is given by Equation 7.4.

$$\Delta OC = (AEC_{baseline\,unit} \ - \ AEC_{design\,option}).EP \qquad (7.4)$$

The annual electricity consumption is obtained by multiplying the ratio of the cooling capacity (Q_{cap}) to the energy efficiency ratio (*EER*) with the annual operating hours (*AOH*) of the equipment. It can be determined using Equation 7.5.

$$AEC = \frac{Q_{cap}}{EER}.AOH \qquad (7.5)$$

The annual operating hours of air-conditioning unit shall vary from place to place within a country based on the environmental conditions. It also varies based on the size of the unit and the proper sizing of the AC unit to the space requirements. Therefore, based on the usual practices and the weather prevailing in the Kingdom of Saudi Arabia the annual operating hours for this analysis was considered to be three thousand and five hundred which constitutes to about forty percent of the annual hours [47].

The illustrations pertaining to the economic analysis presented in the previous section are applied to the air conditioning unit I-III. Consequently, the annual energy consumption (in kW-hr) is calculated and based on the purchasing price, the annual operating hours and the electricity price the pay-back-period for the proposed enhancements is calculated. The pricing of the electricity is done in Saudi Riyals (*SAR*). However, since the electricity pricing in Saudi Arabia is depended on the type of application *i.e.* household, commercial *etc.* and also on the amount of energy consumed. The electricity price per kilowatt-hour was considered in the range of 0.05-0.35 SAR, while the average electricity price for Saudi Arabia lies in the range of 0.15-0.25 SAR/kW-hr. The estimation of pay-back-period also includes the average electricity price in the Europe *i.e.* 0.76 SAR/kW-hr [49] and America *i.e.* 0.42 SAR/kW-hr [50]. The calculated pay-back-period based on the different design option modifications is presented in Table 9.4 to Table 9.6.Table 9.4

Table 9.4 Economic Analysis - Calculation of Pay-Back-Period (Package Unit).

S.no.	Design Option	Pay Back Period (in years)								
		0.05	*0.1*	*0.15*	*0.2*	*0.25*	*0.3*	*0.35*	*0.42*	*0.76*
1	Base line (9.3EER comp)	-	-	-	-	-	-	-	-	-
2	1 + 10% increase in condenser face area	0.31	0.16	0.1	0.08	0.06	0.05	0.04	0.04	0.02
3	2 + 10% increase in evaporator face area	0.54	0.27	0.18	0.13	0.11	0.09	0.08	0.06	0.04
4	3 + 10.1EER comp	2.25	1.13	0.75	0.56	0.45	0.38	0.32	0.27	0.15
5	4 + 10.9EER comp	3.24	1.62	1.08	0.81	0.65	0.54	0.46	0.39	0.21
6	5 + 11.3EER comp	3.65	1.82	1.22	0.91	0.73	0.61	0.52	0.43	0.24

Table 9.5 Economic Analysis - Calculation of Pay-Back-Period (Split Unit)

S.no.	Design Option	Pay Back Period (in years)								
		0.05	*0.1*	*0.15*	*0.2*	*0.25*	*0.3*	*0.35*	*0.42*	*0.76*
1	Base line (9.5EER comp)	-	-	-	-	-	-	-	-	-
2	1 + 10% increase in condenser face area	0.77	0.39	0.26	0.19	0.15	0.13	0.11	0.09	0.05
3	2 + 10% increase in evaporator face area	0.79	0.4	0.26	0.2	0.16	0.13	0.11	0.09	0.05
4	3 + 10.2 EER compressor	2.06	1.03	0.69	0.51	0.41	0.34	0.29	0.25	0.14
5	4 + 10.9 EER compressor	3.44	1.72	1.15	0.86	0.69	0.57	0.49	0.41	0.23

Table 9.6 Economic Analysis - Calculation of Pay-Back-Period (Window Unit)

S.no.	Design Option	Pay Back Period (in years)								
		0.05	0.1	0.15	0.2	0.25	0.3	0.35	0.42	0.76
1	Base line (9.9EER comp)	-	-	-	-	-	-	-	-	-
2	1 + 10% increase in condenser face area	0.98	0.49	0.33	0.25	0.2	0.16	0.14	0.12	0.06
3	2 + 10% increase in evaporator face area	1.27	0.63	0.42	0.32	0.25	0.21	0.18	0.15	0.08
4	3 + 10.0 EER compressor	1.67	0.83	0.56	0.42	0.33	0.28	0.24	0.20	0.11
5	4 + 10.6EER compressor	5.13	2.56	1.71	1.28	1.03	0.85	0.73	0.61	0.34
6	4 + 10.9 EER compressor	5.05	2.53	1.68	1.26	1.01	0.84	0.72	0.60	0.33

9.1 Restrictions on Design Modifications for Performance Improvement

1. Using components that match with each other for efficient functioning of the unit. Improper or poor selection must be avoided at each level of design.

2. The increase in the face area of the heat exchangers has to be restricted to a minimal in order to minimize the changes that have to be incorporated in the manufacturing process and assembly lines.

3. The increase in the purchase cost must be kept nominal by avoiding major changes in the production cycle especially in case of mass production.

CHAPTER 10

IMPACT ON NATIONAL ECONOMY

AND ENVIRONMENT

This section deals with the impact of the technical analysis of the design options on the national economy and the environment. The following analysis is based on the results of the national census and the surveys on the Study of efficient air conditioning and refrigeration technologies. According to the results of the national census of the year 2004 [48] there exist about four million households in the Kingdom of Saudi Arabia. Further, the surveys indicate that only about 75% of these households use air conditioners for cooling. Among these households the average number of room air conditioners per

house is about four units. Moreover, the surveys also indicate the percentages of air conditioning types as window 65%, split 22%, and 13% for packages [48].

Adding up these numbers indicate that the total number of houses that are using window air conditioners are about 1,950,000 units, and those using split air conditioners are around 660,000 units while the houses using the package air conditioners are about 390,000. So, the total number of air conditioning units in use is about 7.8 million window units, 2.64 million split units and 390,000 package units [48].

Based on the numbers indicated above the national level impact of the design options can be estimated. According to the World Energy Council [51], 1000 standard cubic meters of natural gas is equivalent to 36 GJ of energy (net calorific value). Further according to Environmental and Social Statistics, 1 barrel of crude oil is equivalent to 1714 kWh of energy [52]. These values are based only on the heating value of the fuel without taking into consideration the efficiency of energy conversion. In order to estimate the amount of savings in terms of different fuel equivalents, a simple exercise involving the annual energy savings (in kW-hr), calorific value of the fuel (MJ/m^3) [5353-54], and the efficiency of the thermal power plant (η_{plant}) is required. The thermal power plants can be considered to be the most efficient, thereby having a plant efficiency of 40 percent. Further, the carbon dioxide emissions are measured in terms of amount of CO_2 emitted per kWh of the fuel burnt [56]. In this case the fuel considered is natural gas (methane). The national savings in monetary terms (US$) is evaluated by considering the cost of

113

crude oil in the world market [57]. The following tables show the impact of the improvement in the energy efficiency on the national economy and the environment.

Table 10.1 Annual National Savings in Natural Gas Equivalent (standard cubic meters)

Unit	Annual Energy Savings		Annual Savings in Natural Gas Equivalent (cu. mt.)
	per unit (kWh)	Total (GWh)	
Package	4665.5	1,819.55	411,248,242.09
Split	3391.5	8,953.56	2,023,657,458.56
Window	1876.0	14,632.80	3,307,262,682.07

Table 10.2 Annual National Savings in Gasoline Equivalent

Unit	Annual Energy Savings		Annual Savings in US Gallons of Gasoline	Annual Savings in Barrels of Gasoline
	per unit (kWh)	Total (GWh)		
Package	4665.5	1,819.55	122,251,420.12	2,910,748.00
Split	3391.5	8,953.56	601,570,956.01	14,323,118.00
Window	1876.0	14,632.80	983,147,204.59	23,408,267.00

Table 10.3 Annual National Reduction in CO2 Emissions

Unit	Annual Energy Savings		Annual Savings in Natural Gas [Methane] Equivalent (cu. mt.)	Annual Reduction in CO2 emissions (kg)
	per unit (kWh)	Total (GWh)		
Package	4665.5	1,819.55	411,248,242.09	418,496,500.00
Split	3391.5	8,953.56	2,023,657,458.56	2,059,318,800.00
Window	1876.0	14,632.80	3,307,262,682.07	3,365,544,000.00

114

Table 10.4 Annual National Savings in US$

Unit	Annual Energy Savings		Annual Savings in Barrels of Crude Oil	Annual Savings in US$ (millions)
	per unit (kWh)	Total (GWh)		
Package	4665.5	1,819.55	2,741,585.00	191.91
Split	3391.5	8,953.56	13,490,707.00	944.35
Window	1876.0	14,632.80	22,047,858.00	1,543.35

10.1 Results under SASO Testing Conditions

In all the previous chapters, the performance evaluation of the AC units was carried out at ARI testing conditions. In order to depict the effect of the testing conditions on the performance of the air conditioning unit, the thermal performance evaluation of air conditioning units are carried out under SASO testing conditions. The Table 10.5 through Table 10.7 shows the design option modifications for AC unit I, II, and III respectively, under the SASO testing conditions.

Table 10.5 Design Option Modification of AC Unit I (Package Unit) under SASO
Testing Conditions

S.no.	Design Modification	% inc in cost	% inc in EER
1	Base line (9.3 EER compressor)	-	-
2	1 + 10% increase in condenser face area	1.22	0.12
3	2 + 10% increase in evaporator face area	3.19	0.15
4	3 + 10.1 EER compressor	17.31	4.97
5	3 + 10.9 EER compressor	31.22	11.52
6	3 + 11.3 EER compressor	38.14	13.81

Table 10.6 Design Option Modification of AC Unit II (Split Unit) under SASO Testing
Conditions

S.no.	Design Modification	% inc in cost	% inc in EER
1	Base line (9.5EER compressor)	-	-
2	1 + 10.2 EER compressor	10.41	8.59
3	2 + 10.9 EER compressor	20.70	10.56
4	3 + 11.2 EER compressor	25.94	11.74

Table 10.7 Design Option Modification of AC Unit II (Window Unit) under SASO
Testing Conditions

S.no.	Design Modification	% inc in cost	% inc in EER
1	Base line (9.9EER compressor)	-	-
2	1 + 10% increase in condenser face area	3.21	7.63
3	2 + 10% increase in evaporator face area	5.13	10.78
4	3 + 10.0 EER compressor	7.80	12.34
5	4+ 10.6 EER compressor	29.86	17.78

It is clear from the above table that the amount of improvement in the AC performance is less under SASO testing conditions as compared to ARI testing conditions presented in Chapter 9. The less amount of improvement in the AC performance as indicated by the percentage increase in EER is due to the fact that SASO testing conditions are severe than ARI testing conditions.

Since the improvement in the EER under SASO testing conditions is less compared to ARI testing conditions, the amount of annual energy savings for will be less under SASO testing conditions when compared with ARI testing conditions. The Table 10.8 compares the amount of annual energy savings for AC Unit I under ARI and SASO testing conditions.

Table 10.8 Comparison of Annual Energy Savings (Package Unit) under ARI and SASO Testing Conditions

S.no	Type of Saving	Testing condition	
		ARI	SASO
1	Total Annual Energy Savings (GWh)	1,819.55	803.99
2	Annual Savings in Natural Gas Equivalent (cu. mt.)	411,248,242.09	181,714,339.53
3	Annual Savings in US Gallons of Gasoline	122,251,420.12	54,018,069.36
4	Annual Savings in Barrels of Gasoline	2,910,748.00	1,286,145.00
5	Annual Reduction in CO_2 emissions (kg)	418,496,500.00	184,917,700.00
6	Annual Savings in Barrels of Crude Oil	2,741,585.00	1,211,398.00
7	Annual Savings in US$ (million)	191.91	84.79

Table 10.9 Comparison of Annual Energy Savings (Split Unit) under ARI and SASO Testing Conditions

S.no	Type of Saving	Testing condition	
		ARI	SASO
1	Total Annual Energy Savings (GWh)	8,953.56	3,890.04
2	Annual Savings in Natural Gas Equivalent (cu. mt.)	2,023,657,458.56	879,215,469.61
3	Annual Savings in US Gallons of Gasoline	601,570,956.01	261,363,645.49
4	Annual Savings in Barrels of Gasoline	14,323,118.00	6,222,944.00
5	Annual Reduction in CO_2 emissions (kg)	2,059,318,800.00	894,709,200.00
6	Annual Savings in Barrels of Crude Oil	13,490,707.00	5,861,287.71
7	Annual Savings in US$ (million)	944.35	410.29

Table 10.10 Comparison of Annual Energy Savings (Window Unit) under ARI and
SASO Testing Conditions

S.No	Type of Saving	Testing condition	
		ARI	SASO
1	Total Annual Energy Savings (GWh)	14,632.80	8,681.40
2	Annual Savings in Natural Gas Equivalent (cu. mt.)	3,307,262,682.07	1,207,473,631.34
3	Annual Savings in US Gallons of Gasoline	983,147,204.59	358,944,674.01
4	Annual Savings in Barrels of Gasoline	23,408,267.00	8,546,302.00
5	Annual Reduction in CO2 emissions (kg)	3,365,544,000.00	1,996,722,000.00
6	Annual Savings in Barrels of Crude Oil	22,047,858.00	8,049,619.91
7	Annual Savings in US$ (million)	1,543.35	563.47

CHAPTER 11

CONCLUSIONS AND

RECOMENDATIONS

The aim of the present work is to develop a mathematical model for an air conditioning unit with vapor compression refrigeration as its working cycle. The mathematical model is coded into a computer program and the parameters of prime interest are calculated. The overall performance of the air conditioning unit is improved by varying the design parameters such as the condenser face area, evaporator face area, *etc*. The impact of the design option modifications on the national economy and environment is studied.

11.1 Conclusions

The following conclusions can be deduced from the present work:

1. The mathematical model for the air conditioning unit was developed and coded into Engineering Equation Solver, a computer program, to evaluate the thermal performance.

2. The overall performance of the air conditioning unit increases until the condenser face area reaches 14.0, 9.0, and 3.25 sq. ft. for unit I, II and III respectively. Any further increase in the condenser face area does not improve the overall performance of the air conditioning units.

3. The overall performance of the air conditioning unit increases until the evaporator face area reaches 6.0, 5.5, and 2.5 sq. ft. for unit I, II and III respectively. Any further increase in the evaporator face area has no significant improvement on the overall performance of the air conditioning units.

4. The overall performance of the air conditioning unit increases with the increase in the condenser volume flow rate until it reaches an optimum at 2500, 1000, and 275 cubic feet per minute (CFM) for unit I, II and III respectively. Any further increase in the condenser face area decreases overall performance of the air conditioning units.

5. The overall performance of the air conditioning unit increases with the increase in the evaporator volume flow rate until it reaches an optimum at 700, 300, and 275 cubic feet per minute (CFM) for unit I, II and III respectively. Any further

increase in the condenser face area results in a decrease in the overall performance of the air conditioning units.

6. The performance of the compressor also affects the overall performance of the air conditioning units. Such that for units I, II, and III using compressors with EER ranging from 9.3-11.3 Btu/W-hr, 9.5-11.2 Btu/W-hr, and 9.9-10.9 Btu/W-hr respectively. The overall performance varies from 6.74-7.86 Btu/W-hr, 6.98-7.79 Btu/W-hr, and 7.45-8.18 Btu/W-hr respectively.

7. The combinations of the design option modifications results in overall improvement in the performance of the air conditioning unit.

8. The three units studied herein showed an overall increase of 41.79, 32.52, and 28.24% in the EER for the package, split, and window units respectively.

9. The improved in the overall performance resulted in an increase of 38.14, 35.95, and 39.94% in the cost for the package, split, and window units respectively.

10. The estimation of the pay-back-period indicates that the increase in the cost of the AC unit will be recovered in approximately 0.91, 0.86, and 1.26 years for the package, split, and window units respectively at the electricity price of 0.2 SAR/kWh.

11. Based on the national census of the year 2004 the annual total energy savings is estimated to be 25,405.91 GWh. Of which 1,819.55, 8,953.56, and 14,632.80 GWh are accounted for by the package, split and window units respectively.

12. The annual total national savings in terms natural gas equivalent is estimated to be 5,742,168,382.72 cubic meters (std. cu. mt.). Of which 411,248,242.09,

2,023,657,458.56, and 3,307,262,682.07 cu. mt. are accounted for by the package, split and window units respectively.

13. The annual total national savings in terms of gasoline equivalent is estimated to be 41 million barrels. Of which 2,910,748.00, 14,323,118.00, and 23,408,267.00 barrels of gasoline are accounted for by the package, split and window units respectively.

14. The annual total national savings in terms of crude oil equivalent is estimated to be 38 million barrels. Of which 2,741,585.00, 13,490,707.00, and 22,047,858.00 barrels of crude oil are accounted for by the package, split and window units respectively.

15. The annual total national reduction in CO_2 emissions is estimated to be 5.84 million tons. Of which 0.42, 2.05, and 3.37 million tons of reduction in CO_2 emissions are accounted for by the package, split and window units respectively.

16. Lastly, the annual total savings in terms of United Stated Dollars (US$) is estimated to be 2,679.61 million. Of which 191.91, 944.35, and 1,543.35 million US$ are accounted for by the package, split and window units respectively.

11.2 Recommendations

Due to the wide scope of the present work from application point of view, the following recommendations are suggested.

1. Experimental validation of the reported results is needed to be carried out at a psychometric facility.

2. The refrigerant side heat transfer with grooved tubes can be studied.

3. Thermal evaluation of air conditioning units with air-to-water heat transfer can be studied.

Nomenclature

A Area

C_1-C_{10} coefficients of compressor power

$\dot{C}$ Capacitance rate

C_d centre- to-centre distance of bend

Δ refers to change or difference

D Diameter, inside diameter of bend

D_1-D_{10} coefficients of refrigerant mass flow rate

ε Effectiveness

e surface roughness

η Efficiency

E_1-E_{10} coefficients of compressor capacity

EER Energy Efficiency Ratio

f fraction, friction factor

g_c gravitational conversion constant

h Enthalpy, heat transfer coefficient

j Coburn factor

J Mechanical equivalent of heat

k_f Load factor

L length

$\dot{m}$ Mass flow rate

μ dynamic viscosity

NTU	*Number of Transfer Units*
Nu	*Nusselt number*
P	*Pressure*
Pr	*Prandtl number*
q,	*heat transfer rate*
Q	*total heat transfer rate*
ρ	*Density*
Re	*Reynolds number*
T	*Temperature*
U	*Overall heat transfer coefficient*
V	*superficial velocity*
W	*Work done*
x	*vapor mass quality*

Subscripts

Note: Some of these subscripts are also used in combination. For example, atpo refers to air at outlet of two phase section

a	*air*
as	*air side*
b, B	*bend*
comp	*compressor*
c, cond	*condenser*
ci	*condenser inlet*
co	*condenser outlet*

dsh	*de-superheat*
e, evap	*evaporator*
f	*fin, saturated liquid*
g	*saturated vapor, vapor*
HX	*heat exchanger*
in	*inlet*
max	*maximum*
min	*minimum*
out	*outlet*
ref	*refrigerant*
rs	*refrigerant side*
s	*at the surface*
sc	*sub-cool*
st	*straight tube*
tot	*total*
tp	*two-phase*
tpi	*two-phase inlet*
tpo	*two-phase outlet*

References

1. International Energy Outlook, Report #: DOE/EIA-0484(2006); Release Date: June 2006.

2. Najim, A.U., Energy Efficient Buildings and Their Effects on the National Economy, Symposium, King Fahd University of Petroleum and Minerals, 5 Feb. 2002.

3. Saudi Arabian Monetary Agency (SAMA), Forty-Third Annual Report, Research and Statistics Department, (1428H) 2007.

4. Sanaye S. and Malekmohammadi H. R., Thermal and economical optimization of air conditioning units with vapor compression refrigeration system, Applied Thermal Engineering, 24 (2004) 1807–1825.

5. Zhang G. Q., Wang L., Liu L., Wang Z., Thermo economic optimization of small size central air conditioner, Applied Thermal Engineering, 24 (2004) 471–485.

6. Al-Otaibi D.A., Dincer I., Kalyon M., Thermo economic optimization of vapor compression refrigeration systems, Int. Comm. Heat and Mass Transfer, Vol. 31, No. 1, pp. 95- 107, 2004.

7. Ding G. L., Recent developments in simulation techniques for vapor - compression refrigeration systems, International Journal of Refrigeration, 30 (2007) 1119-1133.

8. Morrison G. L., Air Conditioner Performance Rating, Air conditioning - the next 5 years, Asia Pacific Economic Co-operation conference, Sydney 2004.

9. Duprez M. E., Dumont E., Fre`re M., Modeling of reciprocating and scroll compressors, International Journal of Refrigeration, 30 (2007) 873-886.

10. Chen Y., Halm N. P., Groll E. A., Braun J. E., Mathematical modeling of scroll compressors — part I: compression process modeling, International Journal of Refrigeration, 25 (2002) 731–750.

11. Chen Y., Halm N. P., Braun J. E., Groll E. A., Mathematical modeling of scroll compressors — part II: overall scroll compressor modeling, International Journal of Refrigeration, 25 (2002) 751–764.

12. Air-conditioning and Refrigeration Institute (ARI) Standard 540, Performance rating of positive displacement refrigerant compressors and compressor units, 2004.

13. Byun J. S., Leeb J., Choi J. Y., Numerical analysis of evaporation performance in a finned-tube heat exchanger, International Journal of Refrigeration, 30 (2007) 812-820.

14. Domanski P.A., EVSIM an evaporator simulation model accounting for refrigerant and one dimensional air distribution, NIST report, NISTIR 89-4133, 1989.

15. Wang C.C., Chi K.Y., Heat transfer and friction characteristics of plain fin-and-tube heat exchangers, part I: new experimental data, International Journal of Heat and Mass Transfer, 43 (2000) 2681-2691.

16. Wang C.C., Chi K.Y., Chang C.J., Heat transfer and friction characteristics of plain tube heat exchangers, part II: Correlation, International Journal of Heat and Mass Transfer, 43 (2000) 2693-2700.

17. Wang C.C., Jang J.Y., Chiou N.F., A heat transfer and friction correlation for wavy fin and tube heat exchangers, International Journal of Heat and Mass Transfer, 42 (1999) 1919-1924.

18. Wang C.C., Lee C.J., Chang C.T., Lin S.P., Heat Transfer and friction correlation for compact louvered fin and tube heat exchangers, International Journal of Heat and Mass Transfer, 42 (1999) 1945-1956.

19. Wang C.C., Tao W.H., Chang C.C., An investigation of the airside performance of the slit fin and tube heat exchangers, International Journal of Refrigeration, 22 (1999) 595-603.

20. Pierre B., Flow Resistance with Boiling Refrigerants-Part I, ASHRAE Journal 6, No. 9, p 58-65, September 1964.

21. Pierre B., Flow Resistance with Boiling Refrigerants-Part II, ASHRAE Journal 6, No. 10, p 73-77, October 1964.

22. Geary D. F., Return bend pressure drop in refrigeration system, ASHRAE Transactions; 8(1):25064, 1975.

23. Yang L., Wang W., A generalized correlation for the characteristics of adiabatic capillary tubes, International Journal of Refrigeration, 31 (2008) 197–203.

24. Crane, Crane Technical Paper 410, Flow of Fluids thorough Valves, Fittings, and Pipe, twenty four printing, Crane Company 1988.

25. Choi J., Kim Y., Kim H. Y., A generalized correlation for refrigerant mass through adiabatic capillary tubes, International Journal of Refrigeration, 26 (2003) 881–888.

26. Zhou G., Zhang Y., Numerical and experimental investigations on the performance of coiled adiabatic capillary tubes, Applied Thermal Engineering, 26 (2006) 1106–1114.

27. Chuan Z., Shanwei M., Jiangpin C., Zhijiu C., Experimental analysis of R22 and R407c flow through electronic expansion valve, Energy Conversion and Management, 47 (2006) 529–544.

28. Park C., Cho H., Lee Y., Kim Y., Mass flow characteristics and empirical R22 and R410A flowing through expansion valves, International Journal of Refrigeration, 30 (2007) 1401-1407.

29. Buckingham E., On physically similar systems: illustrations of the use of dimensional equations, Physics Rev., 4(4) (1914) 345-76.

30. Mc Quiston, Face C., Heating, Ventilation, and Air Conditioning, 6th ed., John Wiley & Sons, Inc., New York, 1977.

31. Wang K. S., Handbook of Air Conditioning and Refrigeration, McGraw-Hill, Inc., New York, 1994.

32. Moran M. J., Shapiro H. N., Fundamental of Engineering Thermodynamics, 2nd ed., John Wiley & Sons, Inc., New York, 1992.

33. Shapiro H.N., Semi-Empirical Method for Modeling a Reciprocating Compressor in Refrigeration systems, ASHRAE Transactions, 1995.

34. Stoecker W. F., Proposed procedures for simulating the performance of components and systems for energy calculations, American Society of Heating Refrigeration and Air Conditioning Engineers, New York, 1971.

35. Bourdouxhe J. P., Grodent M., Lebrun J., HVAC1KIT, A Toolkit for Primary HVAC System Energy Calculation, 1995.

36. Reichler M., Modeling of Rooftop Packaged Air Conditioning Equipment, Master's Thesis, University of Wisconsin, Madison, 1999.

37. Braun J. E., Klein S. A., Mitchell J. W., Effectiveness Models for Cooling Towers and Cooling Coils, ASHRAE Transactions, Volume 95, Part 2, 1989.

38. Incropera F. P., and de Witt, D. P., Introduction to Heat Transfer, John Wiley & Sons, Inc., New York, 1996.

39. Traviss D. P., Rohsenow W.M., Baron, A. B., Forced convection condensation inside tubes: a heat transfer equation for condensation design, ASHRAE Transactions, 79(1) (1973) 157-165.

40. Chaddock J., B., Noerager J., A., Evaporatoion of R-12 in a horizontal tube with constant wall heat flux, ASHRAE Transactions, 72(1) (1966) 90-102.

41. American Society of Heating, Refrigerating and Air-Conditioning Engineers (ASHRAE) Handbook, Fundamentals, CD-Rom 1997.

42. Kuehl S., J., Goldschmidt V., W., Steady flows of R-22 through capillary tubes: test data, ASHRAE Transactions, 104 (1996) 719-728.

43. Vennard, Elementary Fluid Mechanics, fourth edition, John Wiley & Sons, Inc., New York, London, 1961.

44. Streeter-Wylie, Fluid Mechanics, eighth edition, McGraw Hill, Inc., New York, 1985.

45. Emerson Climate Technologies- Heating, Air Conditioning and Refrigeration Solutions, Compressor performance Data Sheets, 2008.

46. Danfoss Commercial Compressors (DCC), Danfoss Manueurop, Compressor performance data sheets (ODSG), 2008.

47. Mokheimer M. A. Esmail, Said S. M. Syed, Project#SB050021, Survey on Estimation of the annual number of operating hours of Air conditioners for cooling, King Fahd University of Petroleum and Minerals, 2007.

48. Mokheimer M. A. Esmail, Project# CER02321, Study of Efficient Air Conditioning and Refrigeration Technologies, Centre for Engineering Research, Research Institute, King Fahd University of Petroleum and Minerals, Dhahran, June 2008.

49. Goerten J., Clement, E., Electricity prices for EU households and industrial consumers on 1st January 2007, Catalogue number: KS-SF-07-080-EN-N, Eurostat, June 2007.

50. Energy Information Administration, Form EIA-826, "Monthly Electric Sales and Revenue Report with State Distributions Report". Report Number: DOE/EIA-0226 (2009/04), April 2009.

51. Survey of Energy Resources, World Energy Council, Conseil Mindial De L'Energie, 2007.

52. OECD Fact book 2005 Economic, Environmental and Social Statistics http://thesius.sourceoecd.org/vl=9623943/cl=36/nw=1/rpsv/factbook/11-01-01.htm.

53. Calorific value of fuels, http://www.engineeringtoolbox.com/fuels-higher-calorific-values-d_169.html.

54. Calorific values of liquid fuels, http://www.eppo.go.th/ref/UNIT-OIL.html.

55. Density of Liquid fuels, http://www.simetric.co.uk/si_liquids.htm.

56. Amount of CO_2 emissions based on the type of fuel burnt http://www.engineeringtoolbox.com/co2-emission-fuels-d_1085.html.

57. Crude Oil price of US Oil, Arab News, www.arabnews.com, June 28, 2009.

VITAE

Name: Syed Hussain

Contact Address: H.no: 2-3-304 to 307, Flat# 403

RM HRA Apartments, Ramgopalpet

Nallagutta, Secunderabad 500003

Phone: +91-40-27848216, +966-568488374

Email: hussain_says@yahoo.com

syedhussain@kfupm.edu.sa

Date of Birth: 03 June 1984

Education: Master of Science May 2009

Department of Mechanical Engineering

King Fahd University of Petroleum & Minerals

Dhahran-31261, Saudi Arabia

Bachelor of Engineering May 2005

Department of Mechanical Engineering

Muffakham Jah College of Engineering & Technology

Osmania University

Hyderabad, India